The Astrophysical Journal, 315:104–121, 1987 April 1

MOLECULAR CLOUDS AND THE GOULD BELT

David K. Taylor and R. L. Dickman
Department of Physics and Astronomy and Five College Radio Astronomy Observatory, University of Massachusetts

AND

N. Z. Scoville
Department of Physics and Astronomy and Five College Radio Astronomy Observatory, University of Massachusetts, and Department of Astronomy, California Institute of Technology

Received 1985 November 8; accepted 1986 September 23

ABSTRACT

We investigate the relationship of the local system of molecular clouds to the Gould belt. A careful examination of the National Geographic–Palomar Observatory Sky Survey Atlas (POSS) yielded a catalog of dark clouds with accurately measured positions as far south as $\delta = -27°$. From a nonlinear least squares fit to these data, along with positions from Feitzinger and Stüwe's catalog of southern clouds, we find a subset of dark clouds to be distributed irregularly along a curve $b = -3.5° + 12.5° \sin(l - 27.5°)$. This is similar to the distribution of the system of O and B stars used to define the system.

Radial velocities in the $J = 1 \rightarrow 0$ transition of carbon monoxide were measured for all dark clouds in our catalog using the 14 m antenna of the Five College Radio Astronomy Observatory. The velocity distribution of those clouds judged to be members of the belt population suggests an expansion similar to that seen in the neutral atomic hydrogen and OB stars. Similar expansion energies are found for both gas constituents, atomic and molecular, as well as for the Gould belt stars. The velocity-longitude data for our molecular clouds were fitted to a model ring expanding under the influence of Galactic differential rotation and interstellar drag, with poor results. We discuss the reasons for this.

Because the similar expansion energies of the stellar, H I, and molecular gas constituents of the Gould belt are all approximately equal, we suggest that the belt originated in an acceleration of gas rather than in a violent impulse such as a blast wave from one or more supernovae.

Subject headings: galaxies: Milky Way — galaxies: structure — interstellar: molecules

I. INTRODUCTION

The Gould belt is a ring of O and B stars inclined approximately 18° to the Galactic plane and lying within about 1 kpc of the Sun. The belt has been investigated in many ways for many years (extensive historical reviews are given by Stothers and Frogel [1974], hereafter SF, and by Frogel and Stothers [1977], hereafter FS). One of the earliest dynamical studies of the system was made by Oort (1927), who pointed out that bright B stars are characterized by a peculiar velocity of ~ 5 km s^{-1}. Eggen (1961) later calculated positions and velocities of 280 O and B stars and concluded that a velocity gradient of about 40 km s^{-1} kpc^{-1}, in part due to expansion, existed across the system in the direction of the Galactic anticenter. The theory of expanding groups was applied to the system by Bonneau (1984), and an expansion age of 40×10^6 yrs (40 Myr) was found. Lesh's (1968) calculation using 294 stars with well-determined distances of less than 600 pc yielded an expansion age of 90 Myr when both field stars and those in associations were modeled. When only those stars belonging to associations were used, however, a lesser age of 45 Myr was determined.

The relationship of the interstellar medium (ISM) to the Gould belt has only recently been investigated. Lindblad (1967) reported the presence of an apparently local neutral hydrogen feature from 21 cm data, which he named feature A. He concluded that the large extent of feature A in Galactic longitude, as well as its positive radial velocity, implied an overall expansion. Lindblad *et al.* (1973) subsequently fitted feature A to a model of an expanding neutral hydrogen shell in a field of Galactic differential rotation. They obtained an age of 60 Myr and an initial expansion velocity of 3.6 km s^{-1}. They also found that the ring was expanding from a point 140 pc distant from the Sun in the direction $l = 150°$. Hughes and Routledge (1972) examined OH in several nearby clouds and found evidence for an expansion at a slightly larger velocity, about 10 km s^{-1}. Olano (1982) fitted Lindblad's 21 cm data to a refined expanding ring model which included braking forces that would slow the ring as it swept up matter. Olano deduced an age of 30 Myr and concluded that the origin of the system is 166 pc away from the Sun in the direction $l = 131°$.

The research reported in this paper attempts to ascertain whether some molecular clouds in the solar neighborhood can also be considered to be associated with the Gould belt. Section II describes our data-gathering procedure. In § III we determine whether molecular material in the solar neighborhood can be described by two distributions, as is the case for the OB stars, one associated with the Gould belt and one with the Galactic plane. We then attempt to fit the observed radial velocities of the clouds judged to belong to the Gould belt to the model of Olano (1982), in order to clarify the present structure of the system and to chart its evolution. However, the fits obtained for a wide variety of model parameters are poor, leading us to conclude that our data do not fit a unique, unambiguous configuration. In § IV we discuss models for the formation of the Gould belt and critically assess the impact of our molecular cloud data on these models. Also provided is an Appendix which catalogs the 662 molecular clouds observed in this work. We tabulate coordinates, velocities, membership in either the Gould belt or the Galactic belt, and, where possible, cross-reference Lynds (1962) catalog designations for the clouds.

II. OBSERVATIONS

In order to observe CO emission from regions near the Galactic plane, it is first essential to have an accurate representation of the local distribution of dark matter. Although the Lynds catalog of dark nebulae (Lynds 1962) is quite extensive in coverage, cloud coordinates are sometimes in error (e.g., Lynds 1535 is 14′ north of its published position). To acquire a satisfactory list of observing locations, we therefore inspected the POSS prints for dark clouds. Outline tracings were made, and coordinates were measured using the Ohio State overlays (Dixon 1981). Whenever possible, the centers of the most opaque condensations were always chosen for observation. However, in large clouds there is often no preferred central observing location, and in such cases two or more observing sites were chosen, somewhat subjectively, across the cloud. The portion of the sky scanned is bounded by $|b| \leq 24°$ and extends as far south as declination $-27°$, the southern limit for the subsequent radio observations. This guarantees coverage of almost all dark clouds within the Galactic longitude range spanned by the POSS, although an occasional isolated cloud may have escaped detection (e.g., Lynds 183 region). Deliberately avoided for direct observation were bright, somewhat confused areas such as H II regions and reflection nebulae, since one cannot always be certain as to the proper interpretation of a measured spectral radial velocity. However, any dark clouds neighboring H II regions, and therefore potentially associated with the bright nebulae, were observed. Since H II regions typically occupy only a modest fraction of the volume of their parent molecular clouds, we can then be confident that our cloud sample is not significantly biased—either in position or radial velocity—against sites of OB star formation. A list of 730 observing locations was compiled in this fashion. The clouds in this listing generally correspond most closely to Lynds opacity classes 4, 5, and 6 (the most opaque).

Observations of the $J = 1 \rightarrow 0$ transitions of CO and ^{13}CO (rest frequencies 115.3 and 110.2 GHz, respectively) were made in February 1983, May 1983, and February 1984 using the 14 m antenna of the Five College Radio Astronomy Observatory (FCRAO).[1] Fewer than 20% of the clouds were observed in the rarer species. ^{13}CO was used only when marginal weather conditions made the lower sky opacity (and thus system temperature) at 110 GHz sufficiently attractive to compensate for the lines' relative weakness compared to the common isotopic species. The half-power beamwidth of the antenna was approximately 46″ at the higher frequency, with a main beam efficiency of about 50% at both frequencies. The cooled Schottky mixer receiver used for the observations had a single-sideband noise temperature of about 200 K measured at the input of the quasi-optical system. In all observations, a sideband filter with a cryogenic image termination was tuned for single-sideband operation in order to improve calibration accuracy.

Using a 10 MHz local oscillator separation, all spectra were frequency switched. When folded, this yielded a $\sqrt{2}$ improvement in signal-to-noise ratio in the data. Three spectrometers, two with 256 channels × 250 kHz filter width, and one with 256 × 100 kHz filter width, were used simultaneously for the observations. The integration time for each observing position was 60 s for both ^{13}CO and CO, producing a typical rms noise level of 0.8 K in the 250 kHz spectra after folding. Inspection of each cloud spectrum verified that confusion from the ~ 0.5 K telluric CO line was not a problem, as these lines were typically ~ 30 km s^{-1} away from the source emission.

Spectral line intensities, calibrated in terms of antenna temperature by the chopper wheel method (Penzias and Burrus 1973), are believed accurate to better than 30%. However, since the only measurements desired in this program were the radial velocities of the spectral lines, antenna temperature considerations are, in any case, incidental. Based on the signal-to-noise ratio of our data, we estimate the typical error in determining the radial velocities of the clouds to be ≤ 0.4 km s^{-1} in the 250 kHz spectrometer (Dickman and Kleiner 1985).

From the 730 observations made, 662 yielded detections at or above a minimum signal-to-noise ratio of 3:1. Given the care with which the sources were selected, the detection rate of 91% is seemingly low (cf. Dickman 1975). However, in most cases, the sources not seen represent ^{13}CO nondetections in the outer areas of the larger regions of obscuration; there seems little doubt that reobservation in CO would have yielded a detected line in most instances. But given the size of the data base, it was deemed unnecessary to associate a radial velocity with every observing location, and the 68 positions were not reobserved.

III. ANALYSIS

a) *Spatial Distribution*

In Figure 1 we plot in Galactic coordinates the center positions of the 662 clouds detected in either CO or ^{13}CO. Also shown are the clouds south of $\delta = -27°$ tabulated by Feitzinger and Stüwe (1984). Except for the inclusion of the southern data, this figure is quite similar to that shown by Lynds (1968).

It is clear that the clouds are not spread across the sky in a uniform fashion, either in Galactic longitude or, more important, in Galactic latitude. With the Sun only ~ 10 pc from the midplane of the Galaxy (Allen 1976) and the scale height of molecular clouds, σ_{mc}, about 75 pc (Sanders, Solomon, and Scoville 1984), one can expect half of the local dark cloud population (i.e., clouds within 400 pc; see Feitzinger and Stüwe 1986) to be found within $\sim 10°$ of the Galactic plane, assuming a decrease in cloud numbers away from the plane of the form $n = n_0 \exp(-|z|/\sigma_{mc})$. Likewise, given the proximity of our sample of molecular clouds relative to Galactic distances, a fairly uniform distribution in Galactic longitude might be expected. Instead, in the direction of the Galactic center, many clouds lie preferentially above the Galactic plane, while toward the anticenter clouds appear to be distributed mainly below the plane. This is quite similar to the distribution of OB stars which define the Gould belt. In Figure 2 we show the curves describing the Gould and Galactic belts derived by SF for the OB stars, given by $b_{\rm Gould}(l) = (18° \pm 1) \sin [l - (295° \pm 1)]$ and $b_{\rm Gal}(l) = (-3° \pm 0.4) + (5° \pm 1) \sin [l - (149 \pm 7)]$. Also included are our curves describing the distribution of dark clouds. They were derived as follows.

To test whether some clouds have an inclined, planar distribution, we employed a technique similar to the one used by SF. We *assumed* two superposed cloud distributions, one for the Gould belt and one for the Galactic belt. Each is assumed

[1] FCRAO is operated with support from the National Science Foundation under grant AST82-12252 and by permission of the Metropolitan District Commission, Commonwealth of Massachusetts.

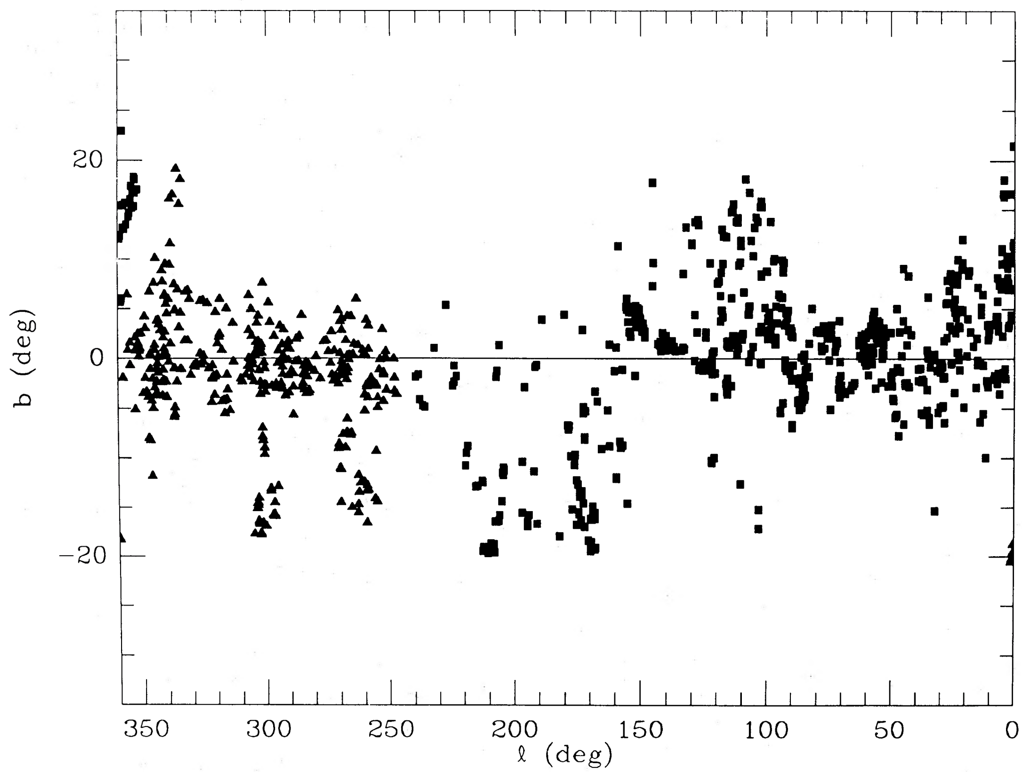

FIG. 1.—Distribution in Galactic coordinates of dark clouds cataloged in this work (*squares*). Only locations with CO or ^{13}CO detections are plotted. Triangles are southern clouds from Feitzinger and Stüwe (1984).

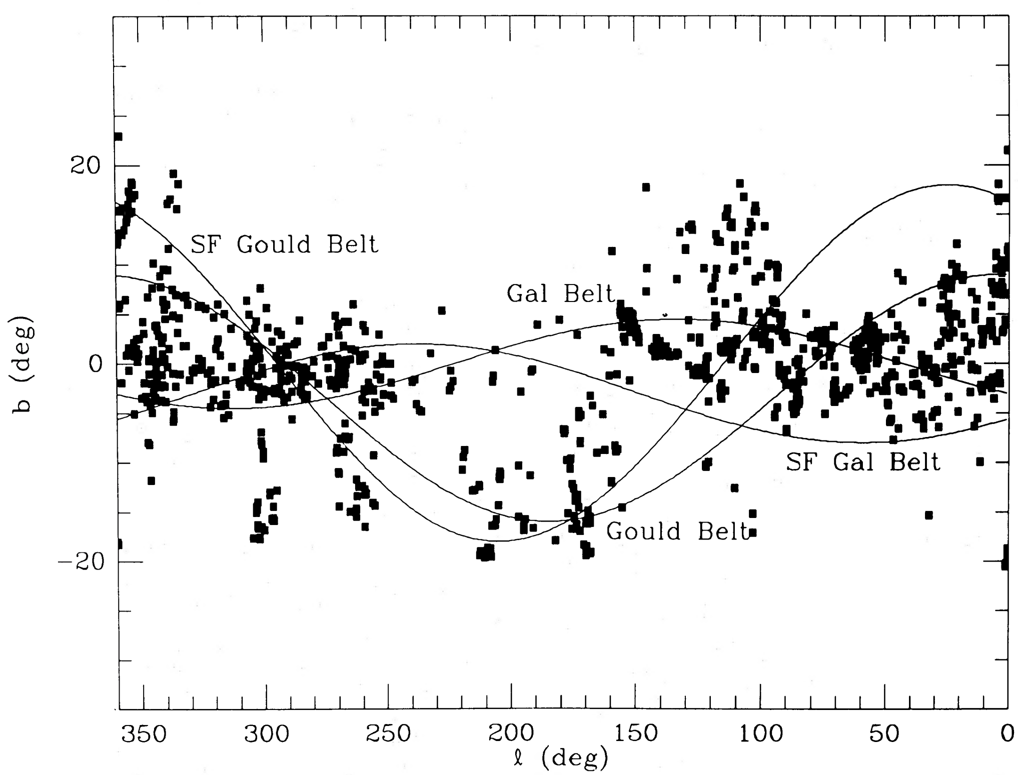

FIG. 2.—Data of Fig. 1 along with curves describing the Gould and Galactic belt OB stars as determined by Stothers and Frogel, as well as corresponding curves for the dark clouds, derived in this work.

to define a plane, given by an equation of the form $b(l) = b_0 + b_1 \sin(l - l_0)$. In order to ascertain the values of the constants b_0, b_1, and l_0 for both belts, an initial guess with $b_0 = 0°$, $b_1 = 15°$, and $l_0 = 270°$ for the Gould belt and $b_0 = 3°$, $b_1 = 5°$, and $l_0 = 149°$ for the Galactic belt was made. Every cloud was then examined for belt membership according to a simple proximity criterion: If the cloud were found to lie closer to the Galactic curve it was included in the Galactic sample; if it lay closer to the midplane of the Gould belt, it was designated a Gould belt member.

After determining the membership status of all clouds, nonlinear least squares fits were done on both samples, in order to determine new best-fit midplane curves. Both subsets of clouds were then recombined, and the new curves used to determine cloud membership again. The procedure was continued until no significant change in either belt membership or the best-fit midplane curves were found. The resulting curves are

$$b_{\rm Gould}(l) = (-3.5° \pm 3) + (12.5° \pm 4) \sin [l - (275° \pm 20)] , \quad (1)$$

and

$$b_{\rm Gal}(l) = (0° \pm 2) + (4.5° \pm 3) \sin [l - (43° \pm 1)] . \quad (2)$$

Owing to the nonlinear nature of the fitting process, it was necessary to verify that solutions (1) and (2) do not depend sensitively upon the initial guesses for b_0, b_1, and l_0. Accordingly, numerous trials were done, with ranges for the Gould belt parameters $-5° \le b_0 \le 5°$, $10° \le b_1 \le 18°$, and $250° \le l_0 \le 290°$; for the Galactic belt these ranges were $-5° \le b_0 \le 5°$, $0° \le b_1 \le 10°$, and $0° \le l_0 \le 360°$. No appreciable difference in the final parameter values was found.

The errors associated with the midplane values of the Gould and Galactic belts, 3° and 2° respectively, are substantial and preclude determining a well-defined displacement of the Sun from the Galactic plane. While clearly very uncertain, the $-3.^{\circ}5$ offset in the Gould curve, however, is consistent with the Sun lying some 10–30 pc above the plane (Allen 1976; Magnani, Blitz, and Mundy 1985).

The 1 σ scatter of 4° for the amplitude of the Gould belt curve defines a characteristic angular thickness for this group of clouds. Unfortunately, without individual distances to the clouds it is imposssible to express this angular measure as a precise physical thickness. However, given that radii of 500 pc or less are characteristically inferred for the stellar Gould belt (SF), and that the local molecular clouds studied here are believed to lie within 400 pc of the Sun (Feitzinger and Stüwe 1986), this 4° scatter suggests a thickness of about 30 pc for the molecular cloud counterpart of the Gould belt. This is significantly smaller than the 75 pc scale height of molecular clouds in the Galactic plane (Sanders, Solomon, and Scoville 1984).

The fact that our catalog of dark nebulae is nearly 3 times smaller than the standard Lynds catalog raises concerns that sheer numerical incompleteness may bias our fits of the two cloud distributions. As a check on the validity of our sample, we therefore repeated the above analysis using the *entire* Lynds catalog, supplemented by the southern clouds of Feitzinger and Stüwe (1984). The resulting Gould belt curve is

$$b_{\rm Gould}(l) = (-2.5° \pm 2.0) + (13° \pm 2.5) \times \sin [l - (263.5° \pm 14.8) , \quad (3)$$

and for the Galactic curve,

$$b_{\rm Gal}(l) = (-1.0° \pm 1.6) + (4.5° \pm 2.2) \sin [l - (28.0° \pm 0.5)] . \quad (4)$$

The very close agreement with equations (1) and (2) suggests that although our sample is roughly one-third the size of the Lynds catalog and is biased toward the most opaque clouds, it is nevertheless sufficient for determining the molecular cloud populations of the Gould and Galactic belts.

A related issue is that it is readily seen in Figure 1 that cloud centers tend to cluster; i.e., the proposed Gould belt members (and indeed the entire cloud sample) are not uniformly spread over the sky. This clustering may lead to improper weighting in the curve fitting. To check this possibility, the analysis was repeated with our 662 cloud positions and the southern clouds grouped into 5° × 5° bins. This resulted in a grid of $72 \times 8 = 576$ squares covering the range $l = 0°$ to $l = 360°$ and from $b = -20°$ to $b = 20°$. A weighted center for each bin was determined by taking the average position of all the clouds that lay within the bin. Bins devoid of clouds were excluded from further analysis. The plane-fitting process outlined above was then repeated, treating the bin centers as if they were themselves clouds. The resulting best-fit curves for the binned sample were

$$b_{\rm Gould}(l) = (-2.5° \pm 5.5) + (12.5° \pm 8) \sin [l - (282° \pm 10)] , \quad (5)$$

and

$$b_{\rm Gal}(l) = (0° \pm 5) + (6° \pm 7) \sin [l - (47° \pm 1)] . \quad (6)$$

The excellent agreement between equations (1) and (5) and equations (2) and (6) indicates that we may safely assume that data clustering has a negligible effect on our best-fit curves.

In Figure 3 we plot our fit to the molecular cloud counterpart of the Gould belt, as given by equation (1). Apart from a (possibly significant) smaller amplitude, the morphology of the molecular cloud system agrees reasonably well in terms of midplane and phase angle with that determined by SF for O and B stars in the Gould belt. It is noteworthy that the molecular system includes both the nearby Taurus clouds ($d \sim 140$ pc, $l \sim 180°$, $b \sim -15°$; Elias [1978]) as well as those in upper Scorpius ($l \sim 0°$, $b \sim 15°$) which also lie near the Sun ($d \sim 180$ pc). As discussed below (§ IV), the inclusion of both molecular complexes in a system with the dimensions usually associated with the stellar Gould belt (diameter ~750–1000 pc) provides a significant constraint on its geometry and structure.

In Figure 4 we plot our fit to the Galactic belt system of molecular clouds. In comparing this result [eq. (2)] with the Galactic plane fitted by SF, we note that although both systems are assigned virtually identical angular tilts (~5°), the two distributions differ appreciably in phase (by nearly 180°) and in midplane value. However, when the much larger errors associated with the molecular cloud determination are taken into account— errors which stem from our lack of distances to individual clouds and from the number of *statistically independent* cloud samples available on the sky—it is clear that these discrepancies are not significant. The midplane offset of $-3°$ found by SF is only 1.5 σ from our fit value of 0°, and the sine wave amplitude given by equation (2) is so ill-determined, that despite its small formal error, the phase value has little meaning.

Clearly seen in Figure 4 are two almost diametrically opposed plumes of dark clouds extending from the Galactic plane. The northern feature ranges between $100° \le l \le 130°$ and extends above the Galactic plane to $b \approx 20°$, while its southern counterpart lies between $295° \le l \le 315°$ and likewise extends toward $b \approx -20°$. The proximity of the plumes to the SF Gould belt (see Fig. 2) might tempt one to conclude that

1987ApJ...315..104T

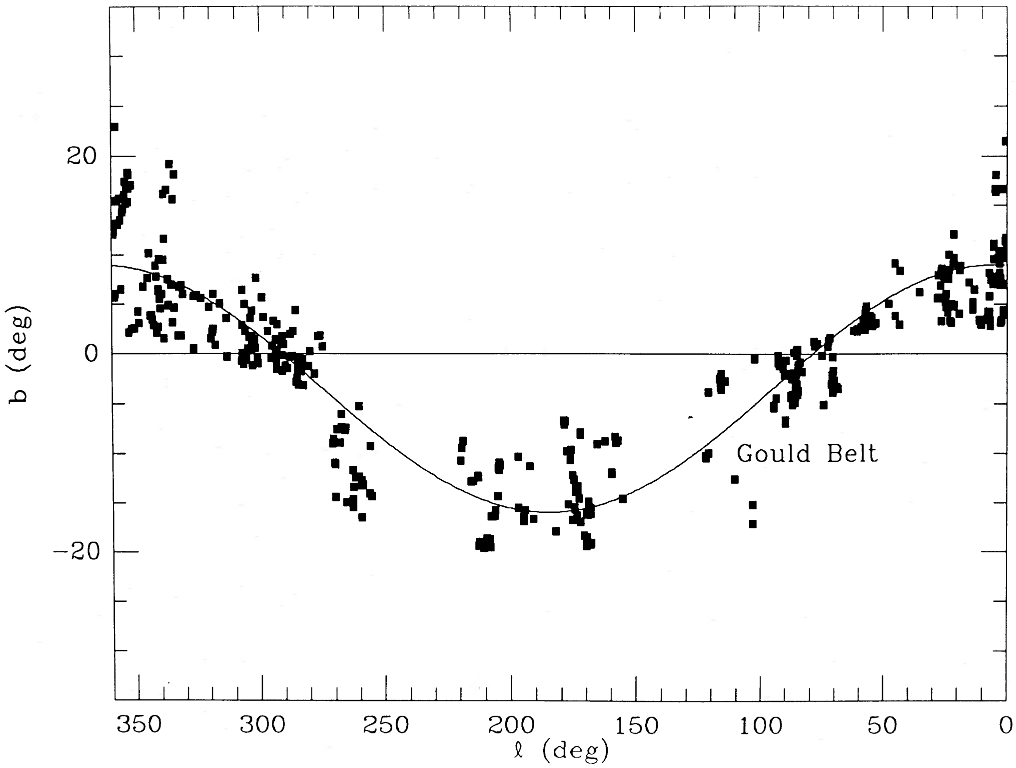

FIG. 3.—Plot of Gould belt clouds and best-fit curve $b = (-3.5° \pm 3) + (12.5 \pm 4) \sin (l = [275° \pm 20])$

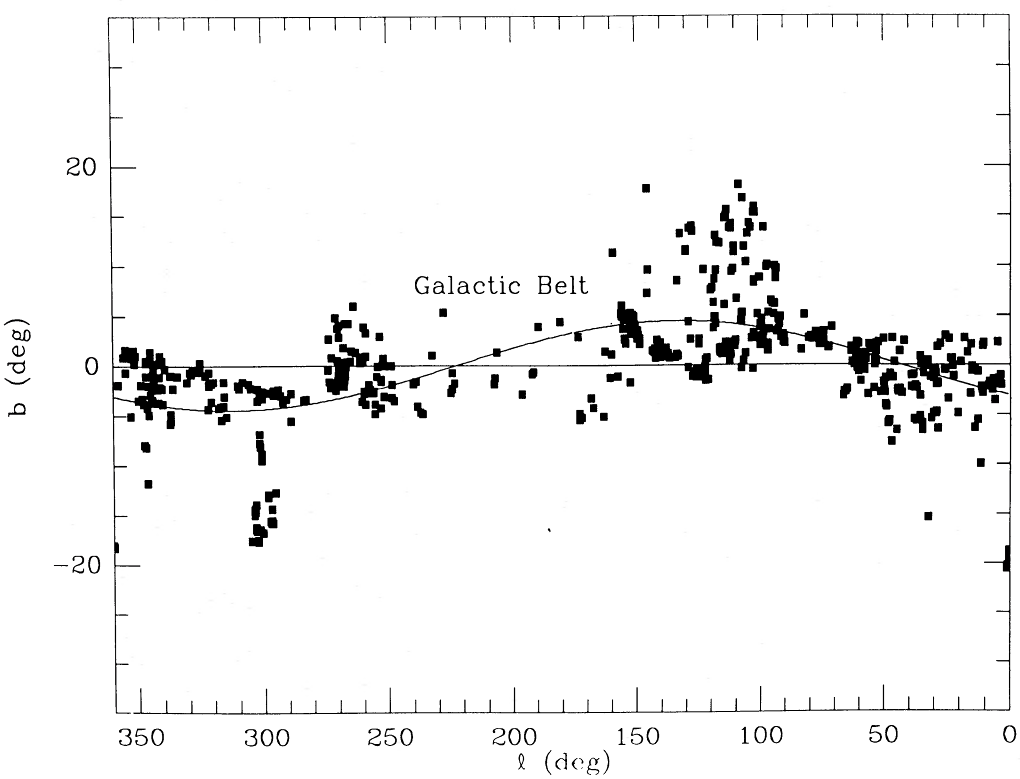

FIG. 4.—Plot of Galactic belt clouds and best-fit curve $b = (0° \pm 2) + (4.5° \pm 3) \sin (l = [43° \pm 1])$

the molecular material of the plumes follows the stellar Gould belt somewhat better than do clouds in most other areas of the sky, and therefore that the molecular clouds of the plumes are closely associated with the OB stars of the Gould belt. However, in the northern plume, the distance to the majority of the clouds in Cepheus is 250–300 pc, and ~300 pc for those clouds in Cassiopeia (Feitzinger and Stüwe 1986). But the Cep OB 2 and Cep OB 3 associations at $l \approx 105°$ are ~700 pc distant (SF), more than twice the distance of the molecular clouds comprising the plume. Therefore, the clouds in the northern feature cannot be associated with the stellar Gould belt and are merely coincident on the sky.

The fact that the two plumes are diametrically opposite on the celestial sphere is intriguing and suggests that they may have originated in the same physical process which shaped the Gould belt (see § IV). It should be noted that the northern plume at least contains relatively little *mass*, the number of sample points shown notwithstanding. This is clearly evident from inspection of Lynds's (1968) map of the local dark cloud system—although the plume's clouds are clearly visible, they possess low mean visual extinction and small total area.

b) *Velocity Distribution*

In the absence of additional systematic motions, one would expect the radial velocities of nearby molecular clouds to follow a pattern consistent with the Schmidt model, i.e., for nearby objects,

$$V_{\rm lsr}(l) = A \cdot d \cdot \sin(2l) , \qquad (7)$$

where A is Oort's constant, equal to 17.7 km s^{-1} kpc^{-1} for $R_0 = 8.5$ kpc (Clemens 1985), and d is the distance to the object. (A coefficient $\cos^2 b$, where b is the Galactic latitude, has been omitted from eq. [7] for clarity. With almost all the clouds in our sample lying between $-12° < b < 12°$, the $\cos^2 b$ factor typically lies between 0.95 and 1.00 and can be omitted.)

Figure 5 shows a velocity-longitude plot for the Gould belt clouds in our sample, along with the velocity curve one would expect for material at a distance of 400 pc. Since the overwhelming majority of dark clouds visible on the POSS are within 400 pc (Feitzinger and Stüwe 1986; the great majority, especially near Taurus and Scorpius are much closer, $d \approx 140$–180 pc), nearly all the clouds would be expected to lie within this curve. The fact that most do not clearly suggests that the observed velocities are not solely due to a differentially rotating galaxy.

Further evidence that this is so comes from the fact that of those clouds assigned to the Gould belt on spatial considerations alone, almost 90% have positive radial velocities. This is shown in Table 1, where we list the percentage of molecular clouds having positive or negative velocities, distinguishing between clouds belonging to the Gould belt or Galactic plane samples. Also, included under the heading "ideal" distribution is the number of clouds in our sample *expected* to have positive or negative velocities, a determination made strictly on the basis of the quadrant of the Galaxy in which they are seen. The simplest explanation for the excess of positive radial velocities is that this represents a definite expansion in the system of local molecular clouds, especially those inclined to the Galactic plane and lying near the Gould belt. The simplest explanation of this motion is that in addition to possessing a spatial dis-

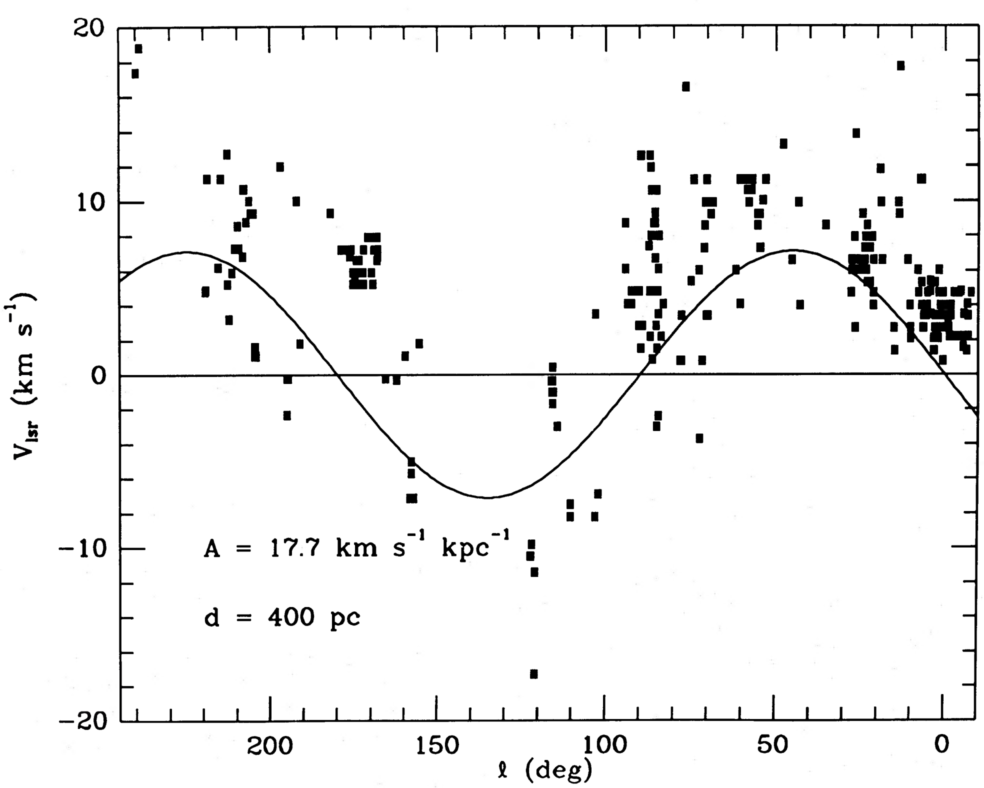

FIG. 5.—$V_{\rm lsr}$ of clouds detected in CO or ^{13}CO vs. Galactic longitude. The curve is not a fit to the data, but rather denotes the $V_{\rm lsr}$ of material in pure differential rotation at a distance of 400 pc from the Sun, assuming Oort's A constant equals 17.7 km s^{-1} kpc^{-1}. See discussion in § III*b*.

TABLE 1

Radial Velocity Distributions

Cloud	Number of Clouds	$V_r > 0$ Observed (%)	$V_r > 0$ Ideal (%)	$V_r < 0$ Observed (%)	$V_r < 0$ Ideal (%)
		All Northern Clouds			
Gould belt	283	89	67 ± 5	11	33 ± 4
Galactic belt	379	60	45 ± 3	40	55 ± 4
All clouds	662	73	54 ± 3	27	46 ± 3
		Binned Sample, Northern Clouds			
Gould belt	65	74	54 ± 9	26	46 ± 8
Galactic belt	90	67	52 ± 8	33	48 ± 8
All clouds	155	70	53 ± 6	31	47 ± 6

tribution reminiscent of the stellar Gould belt, this group of local molecular clouds shares the expansion of the OB stars as well.

It is also evident from Table 1 that the Galactic belt clouds also show an excess of positive velocities, although the imbalance with respect to the ideal case is smaller. This does not necessarily mitigate against a general expansion of the Gould system. Since the Gould belt crosses the Galactic plane at a shallow angle (12°), the area of overlap of the two belts is quite large. Cloud membership assignments in these regions are therefore ambiguous, since they rely on the simple morphological criterion described in § III*a*. Clouds which actually belong to the Gould belt may thus have been assigned membership to the Galactic belt, increasing the number of clouds in that system with positive radial velocity.

It is possible that a fitting algorithm which determines cloud membership with a weight proportional to the belts' widths might result in a Galactic belt sample showing little or no positive radial expansion. This approach, however, has two problems. First, the belt widths would be determined at each iteration step of the fit, as are the belt amplitudes and phases. This could lead to numerical instabilities in the fit. For example, a possible outcome would be the assignment of all the clouds to one belt or the other, and it is even unclear whether such a fit would converge to a unique solution at all. Second, a weighted fit should be carried out using the physical (as opposed to angular) distances of each cloud from the current belt midplane positions. In this respect, we are hindered by uncertainties (factors of 2–3) in the distances to our clouds. These would hide a belt width ratio comparable to the 3:1 found by SF for the Galactic to Gould system.

Again, it is possible that data clustering (cf. § III*a*) have biased these results. To check this, we have included in Table 1 the expected and observed percentages when the velocities are averaged over the 5° × 5° bins of § III*a*. The good agreement between the binned and unbinned samples suggests that our original data base was effectively unbiased from a kinematic standpoint.

c) Numerical Model

As noted in the Introduction, suspicions that a component of the local interstellar gas possesses a morphology and kinematic behavior similar to the stellar Gould system go back to the work of Lindblad (1967). Since then, there have been suggestions that the local molecular gas shares these properties, but the molecular data have been highly limited and fragmentary in their coverage (e.g., Hughes and Routledge 1972). This is unfortunate for two reasons. A major concern with Lindblad's 21 cm analysis, and subsequent kinematic refinements of it such as Olano's decelerated expansion model (1982), is that it is exceedingly difficult to trace the H I feature, dubbed "A" and presumed to represent the hydrogen counterpart of the belt, through the complex 21 cm spectral line emission of more distant Galactic sources. As a result, kinematic study of the local neutral hydrogen system invariably rests upon Lindblad's *fit* to his 21 cm feature "A," and not upon the observational data themselves. Second, by comparing the kinematic behavior of the expanding molecular system and its 21 cm counterpart one can constrain scenarios which attribute a common explosive origin to the expansion (§ IV).

To address these issues, we attempted to determine whether the motions of our molecular clouds are well fitted by the expanding ring model of Olano (1982). However, whereas Olano used a smooth functional fit to Lindblad's 21 cm feature A, we used the Galactic longitudes and radial velocities of those clouds in our data set judged to belong to the Gould belt. Several starting radius and expansion velocity values were chosen for the model system, and up to 10 best-fit solutions were calculated according to Olano's model, each yielding a different location for the Sun. The solutions all failed to converge to a reasonably unique answer, implying that in contrast to the 21 cm case, Olano's expanding ring model is of little value here. Reasons for this are discussed below.

IV. DISCUSSION

In the previous section we have shown that there exists a definite and unique molecular cloud counterpart to the Gould belt, along with a more extensive subset of clouds distributed along the Galactic plane. An excess of positive radial velocities above the expected distribution due to circular Galactic rotation was observed in those clouds found to lie along the belt. Presumably, this is related to the general expansion seen in the early-type stars and diffuse H I clouds comprising the Gould system. However, the fit of our data to the decelerating, expanding ring model of Olano (1982) was poor.

One possible reason for this is that Olano's model assumes a ring of constant height $H = 200$ pc and starting radius R_0, whose axis of symmetry is perpendicular to the Galactic plane and whose center is located in the plane. The model thus implicitly ignores the most salient morphological property of the Gould system—its tilt with respect to the Galactic plane. This may lead to problems in treating cloud deceleration, since a cloud 400 pc distant from the Sun and located at $b = 15°$ is ~ 110 pc from the Galactic plane, well over a molecular cloud scale height (Sanders, Solomon, and Scoville 1984).

However, a more likely reason why the model failed to give consistent results when applied to our CO observations is that from a purely morphological standpoint, Olano's basic model geometry—a thin hoop—is ill-suited to describe the tilted local molecular cloud system. This is readily appreciated if we note that the Taurus dark clouds, while possessing the expected tilt and phase of the Gould belt, are far too close to the Sun at 140 pc (Elias 1978) to share membership with the far more distant Per OB 1 association (~ 500 pc) usually noted as a prominent belt landmark (e.g., Olano 1982), *unless* one discards a hoop-like morphology; the cloud groupings simply lie too close to each other in longitude to be linked by a simple arc which is also simultaneously consistent with the belt's configuration at other longitudes. Studies of the three-dimensional distribution of interstellar extinction in the direction of the anticenter resolve this problem (Gottlieb and Upson 1969), demonstrating that the Taurus clouds lie at the extreme tip of an arm of material which protrudes inward toward the Sun from the Perseus association. Unless this is judged to be a highly exceptional case, we must conclude that rather than the thin, shallow hoop which successfully modeled the H I data, a more general dynamical model should instead have begun with a ring at least partially *filled* with material and stars (SF).

The lack of well-determined distances for most of our molecular clouds precludes treating such a model, and in the remainder of this section we shall exclude Olano's model from further consideration. Instead, we shall focus on the two salient and apparently model-independent features deduced for both the molecular and atomic clouds, as well as for the stellar belt components—their tilt with respect to the Galactic plane and their expansion—and shall explore how they constrain possible origin scenarios.

a) Local Standard of Rest

Although its tilt is indisputable, one can inquire whether a miscalculation of the local standard of rest (LSR) is responsible for the apparent expansion of the Gould system. This is almost certainly not the case for several reasons. The least-squares fit by FS solves for the peculiar motion of the Sun, i.e., the LSR is redetermined. Their results are in excellent agreement with the accepted values of $V_0 = 20$ km s^{-1} toward $l = 57°$, $b = 22°$ (Allen 1976), not only when all stars are included but also when each subset of stars (the Gould belt and the Galactic belt) is separately fitted. In addition, analysis of the local velocity field (Goulet 1984), using a variety of components including H I clouds and B stars, revealed no substantial changes in results when data associated with the Gould belt were omitted. This suggests that while the Gould belt is a major dynamical system close to the Sun, LSR determinations are *not* strongly influenced by it.

However, an additional concern may be the peculiar motion of the LSR as a whole. By determing the rotation curve of the Galaxy in the vicinity of the Sun, Clemens (1985) determined one component of the peculiar velocity of the LSR itself, finding that the LSR has an additional noncircular velocity of ~ 7 km s^{-1} toward $l = 90°$. This is in good agreement with Shuter's (1982) result of 6.8–8.5 km s^{-1}, which also yielded a value of 4–7 km s^{-1} for the *radial* component of the LSR's peculiar velocity. Nevertheless, Shuter (1982) maintains that the LSR is the correct standard of rest for stars and gas within 1–2 kpc of the Sun. With the data in this work lying well within this boundary, we conclude that V_{LSR} accurately describes the velocity of local molecular clouds, and that the expansion is not the artifact of an undetected error in the local standard of rest.

b) Dynamics

In Table 2 we list the major properties of the three components of the Gould system (the derivation of the table is discussed below). Most striking is the similarity in mass and velocity (and therefore, energy) exhibited by the molecular gas, neutral hydrogen, and stars. This, and the fact that the molecular gas tends to at least partially fill the ring defined by the O and B stars (Gottlieb and Upson 1969), may well be the most important considerations in constructing refined future models for the expansion of the Gould belt. If the expansion seen in the stellar and gaseous material is assumed—as is plausible—to have a common origin, it is important to stress that the stars *must* have formed from the gas if the expansion were initiated by a pressure pulse, irrespective of the pulse's detailed nature. This follows from the inability of any astronomically realistic pressure wave to accelerate a mass as pointlike as a star. Furthermore, any pressure mechanism also requires a fairly small system originally, simply because maintaining the phase coherence of the initiating pulse becomes more difficult as the size of the system grows. In one respect, our identification of a molecular component with the Gould system removes a problem which would occur if H I and stars were to alone comprise the expanding configuration, since star formation is not usually believed to proceed directly from neutral atomic gas.

Bruhweiler *et al.* (1980) have argued that the interaction of supernovae and stellar winds from OB associations with the interstellar medium can create supershells which manifest themselves in the form of expanding regions of swept-up material (and, eventually, young stars). If one or more (simultaneous) supernovae were the origin of the observed Gould belt expansion, one would expect an acceleration pulse acting over a relatively short time span. In this situation a cloud's velocity will be inversely proportional to its density

TABLE 2

COMPONENTS OF THE GOULD BELT

System	Age (10^6 yrs)	R (pc)	Morphology	V_{exp} (km s^{-1})	M ($M_\odot$)	E (ergs)
Stars	45–90[a]	500[b]	Filled ring	~ 5[c]	$\sim 5 \times 10^5$ [d]	$\sim 5 \times 10^{49}$
H I[e]	60	~ 600	Ring	~ 5	$\sim 10^6$	$\geq 10^{51}$
Molecular clouds[f]	≤ 60	~ 300	Filled ring[g]	~ 5	$\sim 4 \times 10^5$	$\sim 10^{50}$

NOTES.—(a) Lesh 1968; (b) SF; (c) FS; (d) Total mass of stars of all spectral types (§ IV*b*); (e) Lindblad 1967; (f) This work; (g) See § IV.

and size, $v \sim 1/\rho L$. However, in a gradual expansion, such as expected to be produced by stellar winds, the acceleration drops as $1/r^2$ (Machnik *et al.* 1980). In this case, the velocity will grow as $v \sim (1/L)^{1/2}$. Taking the density and size of a diffuse hydrogen cloud to be $\rho_H \sim 10$ cm^{-3} and $L_H \sim 10$ pc, respectively, and assuming for a molecular cloud $\rho_m \sim 10^3$ cm^{-3} and $L_m \sim 1$ pc (e.g., Spitzer 1978), respectively, one thus gets $v_H/v_m \sim 10$ for an impulsive expansion as in a supernova, and $v_H/v_m \sim (10)^{1/2}$ for a gradual expansion. The similar expansion velocities seen in the molecular material and atomic hydrogen clouds therefore appear to be better represented by a gradual expansion mechanism. Olano has pointed out that to provide the necessary boundary conditions for his 1982 model (origin centered near α Per in the Cassiopeia-Taurus group about 35 Myr ago and $R_0 = 100$ pc and $V_0 = 20$ km s^{-1}) strictly from stellar winds, a supershell created by ~ 30 massive O stars must be postulated. Olano also calculated that to produce identical conditions solely from supernovae, about 10 Type II supernovae would be required. Although this requires a somewhat more modest number of massive stars, because the energy deposition must occur over a short period of time, the supernovae must essentially go off simultaneously. This may be an unrealistic constraint.

A complicating factor in this analysis is the addition of interstellar drag. Since the force of drag goes as $\rho_{ext} v^2 L^2$, where ρ_{ext} is the density of the ambient ISM, larger and higher velocity material (namely the H I clouds) will slow much more than the molecular material. Thus, the velocity ratio $v_H/v_m \sim 3$ of a gradual expansion will be reduced even more; likewise, so will the velocity ratio predicted by an explosive event, possibly to a level consistent with the uncertainties of the present observations. Still further complications arise because the material forming the ring seen today is inclined with respect to the plane of the Galaxy. The quantity ρ_{ext} then depends upon distance from the Galactic plane, and the drag force becomes a bit more complicated to model. To determine whether this has any effect on the fit, the numerical model of § III*c* was repeated using an interstellar density of the form $\rho_{ext} = \rho_0 \exp(-|z|/\sigma_{mc})$, with the model forced to adopt the inclination observed. No significant difference was found between this model and the results shown in Table 2.

As already noted, Table 2 summarizes some important physical parameters for each major component of the Gould system. In compiling the table it was necessary to make several assumptions. To determine a total stellar mass, for example, a stellar mass distribution characteristic of the local Galactic disk population was assumed (Allen 1976) and applied as a normalization factor to the total number of O and B stars tabulated by Lesh (1968) as belt members.[2] In a similar fashion, the molecular cloud mass given was obtained from the total mass of the local dark cloud system estimated by Lynds (1962), scaled by the fractional population of belt clouds in our sample. It should also be recognized that the expansion velocities listed for both gaseous components are almost surely uncertain at the $\pm 50\%$ level.

Despite these uncertainties, at least three important facts emerge from consideration of the Table. First, star-formation efficiency in the belt—some 30% by mass—is significantly higher than the few percent which on average characterize the local ISM. Rates of this magnitude have, however, been reported to pertain to certain active regions such as the core of the ρ Oph molecular cloud (Wilking and Lada 1983). Second, within the uncertainties, the three belt components have essentially equal expansion energies at present. Third, the total observed expansion energy is comparable to the output of a Type II supernova. Since the mechanical coupling of a cloud to an external pressure wave is quite inefficient (e.g., Cox 1979), this implies that unless one postulates a hitherto unobserved sort of object, *any* stellar trigger for the expansion of the Gould system must have involved a multiplicity of high-mass stars. (This has already been mentioned above in connection with the supernova scenario.)

Taken together, all these facts lead us to strongly favor a gradual, rather than catastrophic origin for the expansion of the Gould belt (this may involve either wind or ionization-front driven pressure waves). It is possible (though unproven here) that with suitably chosen model parameters, interstellar drag might reduce the initially large velocity disparity produced by an explosive acceleration of atomic and molecular material. However, while *any* stellar genesis scenario requires on energy grounds the essentially simultaneous *formation* of numerous OB stars—a widely observed phenomenon—the supernova hypothesis alone also requires the simultaneous *detonation* of several stars in order to maintain a coherent expansion over the ring. This appears to be unlikely.

Finally, returning to the expanding ring model, a more complete description would note that there are actually three gaseous components: the ring discussed previously, the two "caps" of gas which move nearly perpendicular to the Galactic plane (Olano 1982). Material ejected toward the Galactic poles by any expansion trigger would meet very little resistance and would essentially undergo simple harmonic motion (if remaining bound to the Galaxy). This material will therefore oscillate about the Galactic plane with frequency $\omega^2 = 5 \times 10^{-30}$ s^{-2}. With the initial conditions of $Z_0 = 100$ pc and $\dot{Z}_0 = 20$ km s^{-1} suggested by Olano (1982), this material should now be falling back toward the plane at about -15 km s^{-1} and would be visible in the direction of the Galactic poles if the age of the system is what Olano determined, 30 Myr. However, if the formation event occurred 40 Myr ago, slightly more than Olano's value and more in keeping with most of the stellar calculations, the material would now be showering back upon the Galactic plane. This may be the origin of the two plumes noted in § III*a*. Perhaps fortuitously, the center of the Gould belt according to Olano's model is at $l = 131°$, close to the center of the northern plume.

V. SUMMARY

We may summarize the results in this paper as follows:

1. A molecular gas component of the Gould belt is found to exist. It is inclined some 12°.5 to the Galactic plane and is offset with respect to the distribution of the O and B stars which define the Gould belt.

2. Carbon monoxide observations of northern clouds show an excess of positive radial velocities in the sample of molecu-

[2] Stothers and Frogel (1974) have observed an enhancement of O–B2 stars over B3–B5 stars in the Gould belt as compared to the local Galactic disk. This may suggest an initial mass function (IMF) for the Gould belt which reflects the formation of high-mass stars at the expense of low-mass stars. Such an IMF would cause our mass estimate in Table 2 to be erroneously high. But the observed enhancement at the high end of the IMF could, in principle, also apply at the low-mass end. Because we have determined the stellar mass of the Gould belt by normalizing a standard IMF with respect to the observed number of O and B stars, this situation would produce no mass error. Until detailed observations of the Gould belt IMF are performed to resolve this question, we regard it as prudent to use a standard IMF.

lar clouds associated with the Gould belt. We attribute this to the expansion of the belt clouds.

3. The positions and radial velocities of the Gould belt clouds were modeled using the expanding ring picture of Olano (1982). No satisfactory fit could be obtained, and hence quantitative constraints on the age and origin of the system were not able to be determined from the model.

4. The H I gas, molecular gas, and stars all have roughly the same mass and expansion velocity. The stars must have formed from the expanding gas, and any stellar trigger for the expansion requires the presence of numerous OB stars. Because of the size and coherence of the belt's expansion, we argue that the expansion is more likely to have been initiated by a gradual acceleration of the clouds, rather than by a violent impulse.

We wish to thank Professor David Van Blerkom for several helpful discussions concerning the dynamics of the Gould system. We also wish to thank the anonymous referee for the many helpful comments and suggestions for improving this paper. This research was supported by NSF grant AST 82-12252 to the Five College Radio Astronomy Observatory. This is contribution number 607 of the Five College Astronomy Department.

APPENDIX

This appendix contains the catalog of dark clouds compiled from our sketches of the POSS prints (Table 3). The clouds listed here correspond most closely to Lynds (1962) opacity classes 4, 5, and 6 (the most opaque). The limits of the sample are $|b| \leq 24°$ and $\delta \geq -27°$. The southern limit of $\delta = -27°$ corresponds to a minimum observing elevation of about 20° from FCRAO.

Although 730 positions were originally recorded and observed, only 662 yielded definite CO or ^{13}CO velocities (see § II). Only these clouds have been included in this catalog. In some regions, we were not certain as to the boundaries of individual clouds. Therefore, some of the larger clouds were observed at several different locations.

The column headings denote (1) identifying number; (2) Galactic longitude, *l*, in degrees; (3) Galactic latitude, *b*, in degrees; (4) right ascension, R.A., in hours (h), minutes (m), seconds (s); (5) declination, decl. in degrees (°), minutes (′), seconds (″); (6) spectral line centroid radial velocity, V_{LSR}, in km s^{-1} with a typical error less than ± 0.4 km s^{-1} (see § II); (7) assignment to either the Gould belt or the Galactic belt; and (8) Lynds object most likely associated with the dark cloud. An asterisk (*) indicates that the observed velocity implies a nonlocal cloud; these were omitted from analysis in the present work. All coordinates are epoch 1950.

TABLE 3

CATALOG OF DARK CLOUDS

No. (1)	l (2)	b (3)	R.A. (4)	Decl. (5)	Velocity (6)	Belt (7)	Lynds # (8)
1	352.18	17.04	$16^h20^m29^s$	−24°49′56″	4.7	Gould	
2	352.95	16.69	16 23 47	−24 31 19	2.2	Gould	1681
3	352.97	18.07	16 19 21	−23 35 24	3.4	Gould	1687
4	353.25	15.30	16 29 16	−25 13 25	4.1	Gould	1689
5	353.38	18.27	16 19 51	−23 09 40	1.4	Gould	
6	353.93	16.90	16 25 49	−23 40 59	2.2	Gould	1704
7	354.31	15.17	16 32 37	−24 32 02	3.5	Gould	
8	354.42	17.41	16 25 29	−22 59 37	1.6	Gould	
9	354.80	16.05	16 31 00	−23 36 07	2.2	Gould	1709
10	355.27	14.69	16 36 51	−24 07 50	4.8	Gould	
11	355.73	14.29	16 39 37	−24 04 28	4.7	Gould	1729
12	356.50	13.47	16 44 17	−23 58 53	4.7	Gould	1745
13	356.90	15.73	16 37 41	−22 15 16	2.2	Gould	1744
14	357.31	13.04	16 47 53	−23 37 38	4.7	Gould	1750
15	357.80	15.45	16 40 59	−21 45 28	2.2	Gould	1755
16	358.08	13.20	16 49 21	−22 56 15	3.4	Gould	1759
17	358.19	22.91	16 17 36	−16 43 13	4.0	Gould	
18	358.52	15.42	16 42 56	−21 14 09	2.2	Gould	1765
19	358.67	6.02	17 16 24	−26 43 13	3.4	Gould	1767
20	358.79	5.66	17 18 00	−26 49 56	2.7	Gould	1773
21	359.00	12.41	16 54 26	−22 42 06	2.9	Gould	1779
22	359.53	12.06	16 57 00	−22 30 12	2.7	Gould	1791
23	0.08	11.14	17 01 37	−22 36 54	4.0	Gould	1802
24	0.25	11.72	17 00 00	−22 07 50	2.7	Gould	4
25	0.45	11.43	17 01 31	−22 08 57	2.7	Gould	15
26	0.49	21.45	16 27 59	−16 00 44	0.8	Gould	1
27	0.53	10.34	17 05 33	−22 43 13	4.7	Gould	20
28	1.08	10.03	17 08 00	−22 27 34	3.4	Gould	32
29	1.24	9.91	17 08 48	−22 24 13	3.4	Gould	39
30	1.35	3.98	17 30 57	−25 42 06	4.0	Gould	42
31	1.40	4.39	17 29 10	−25 23 06	3.4	Gal	52
32	1.50	7.09	17 19 32	−23 47 42	3.4	Gould	55
33	1.54	9.71	17 10 14	−22 16 46	4.7	Gould	51
34	1.77	6.97	17 20 36	−23 38 45	4.7	Gould	
35	1.86	16.64	16 47 11	−17 56 39	6.0	Gould	62
36	1.95	9.88	17 10 38	−21 51 03	2.1	Gould	65
37	1.95	9.80	17 10 56	−21 53 38	3.4	Gould	67
38	2.25	3.37	17 35 00	−25 13 02	3.4	Gould	74
39	2.45	9.82	17 12 04	−21 28 41	2.7	Gould	79
40	2.49	7.07	17 22 00	−22 59 37	2.7	Gould	81
41	2.66	7.66	17 20 18	−22 31 39	2.7	Gould	91
42	2.71	3.16	17 36 53	−24 56 39	3.4	Gould	90
43	2.74	7.01	17 22 49	−22 49 33	2.7	Gould	85
44	2.91	7.43	17 21 42	−22 27 11	5.3	Gould	
45	2.97	9.13	17 15 45	−21 26 47	3.4	Gould	99
46	3.02	8.20	17 19 13	−21 55 52	2.7	Gould	102
47	3.07	9.96	17 13 05	−20 54 04	1.4	Gould	104
48	3.30	10.42	17 12 00	−20 27 14	1.4	Gould	111
49	3.43	7.52	17 22 36	−21 58 06	2.1	Gould	112
50	3.48	−1.99	17 58 15	−26 56 39	10.5	Gal	
51	3.88	−1.04	$17^h55^m27^s$	−26°07′26″	6.0	Gal	133
52	4.03	−1.48	17 57 31	−26 13 02	7.9	Gal	
53	4.23	18.07	16 48 00	−15 16 23	3.5	Gould	137
54	4.50	16.39	16 54 18	−16 03 21	4.8	Gould	
55	4.52	16.62	16 53 32	−15 54 24	5.4	Gould	146
56	4.56	−1.92	18 00 24	−25 58 29	8.6	Gal	
57	4.80	−1.43	17 59 00	−25 31 39	7.9	Gal	
58	5.01	2.29	17 45 24	−23 26 50	6.6	Gal	
59	5.30	11.11	17 14 18	−18 26 27	4.0	Gould	173
60	5.30	10.80	17 15 23	−18 36 31	4.7	Gould	175
61	5.35	9.60	17 19 43	−19 14 32	4.0	Gould	177
62	5.44	7.04	17 29 02	−20 34 17	3.4	Gould	178
63	5.71	7.80	17 26 55	−19 55 32	3.4	Gould	
64	5.96	−1.81	18 03 01	−24 42 06	8.6	Gal	
65	6.26	−3.52	18 10 15	−25 16 46	2.7	Gal	198
66	6.30	7.42	17 29 37	−19 38 22	3.4	Gould	
67	6.31	7.50	17 29 23	−19 35 24	2.7	Gould	
68	6.57	3.36	17 44 56	−21 33 53	4.0	Gould	
69	6.66	2.77	17 47 19	−21 47 18	2.7	Gould	
70	6.76	−1.50	18 03 33	−23 51 03	12.5	Gal	
71	6.94	−2.51	18 07 48	−24 11 55	10.5	Gal	221
72	6.95	5.85	17 36 45	−19 56 15	11.2	Gould	219
73	7.00	4.31	17 42 27	−20 42 06	4.0	Gould	
74	7.09	8.19	17 28 40	−18 33 53	5.3	Gould	220
75	7.43	−1.92	18 06 36	−23 28 41	8.6	Gal	227
76	7.52	4.28	17 43 49	−20 17 30	11.2	Gould	235
77	7.95	3.51	17 47 27	−20 18 37	4.7	Gould	
78	8.00	3.47	17 47 42	−20 16 46	6.0	Gould	
79	8.18	−1.70	18 07 20	−22 43 13	9.9	Gal	
80	8.38	−2.10	18 09 17	−22 44 21	11.8	Gal	
81	10.31	3.42	17 52 53	−18 19 21	2.1	Gould	285
82	10.32	2.97	17 54 32	−18 32 46	2.7	Gould	288
83	10.41	2.19	17 57 34	−18 51 03	6.0	Gal	289
84	10.45	3.03	17 54 36	−18 24 13	4.0	Gould	
85	10.83	−2.80	18 16 59	−20 55 08	11.2	Gal	291
86	10.89	1.89	17 59 41	−18 35 24	7.3	Gal	
87	10.93	−2.65	18 16 36	−20 45 51	11.2	Gal	
88	11.11	3.37	17 54 45	−17 39 29	6.6	Gould	302
89	11.11	−2.51	18 16 28	−20 32 26	11.2	Gal	314
90	11.14	3.45	17 54 32	−17 35 44	6.6	Gould	
91	11.45	−2.21	18 16 01	−20 05 35	11.2	Gal	
92	11.63	−9.95	18 46 03	−23 27 34	7.9	Gal	311
93	12.69	−0.65	18 12 44	−18 15 39	5.3	Gal	323
94	12.91	−5.53	18 31 26	−20 21 15	32.7	Gal	
95	13.14	6.51	17 47 42	−14 19 44	17.7	Gould	330
96	13.60	5.20	17 53 20	−14 35 47	9.2	Gould	339
97	13.83	4.50	17 56 21	−14 44 44	9.9	Gould	341
98	13.89	−0.53	18 14 42	−17 08 57	17.7	Gal	
99	14.09	−6.31	18 36 41	−19 39 52	4.7	Gal	344
100	15.03	7.22	17 49 06	−12 20 51	1.4	Gould	360

TABLE 3—*Continued*

No. (1)	*l* (2)	*b* (3)	R.A. (4)	Decl. (5)	Velocity (6)	Belt (7)	Lynds # (8)
101	15.17	−0.59	18ʰ17ᵐ28ˢ	−16°03′21″	19.0	Gal	
102	15.23	7.22	17 49 29	−12 10 48	2.7	Gould	361
103	15.25	−0.12	18 15 55	−15 45 28	16.4	Gal	
104	15.54	2.04	18 08 38	−14 27 57	30.0	Gal	
105	15.68	−2.28	18 26 54	−16 40 56	9.2	Gal	
106	16.94	1.27	18 14 13	−13 36 31	21.6	Gal	
107	18.10	2.74	18 11 13	−11 53 38	26.8	Gal	386
108	18.58	8.90	17 50 18	−08 27 57	6.6	Gould	392
109	19.04	8.48	17 52 42	−08 16 46	9.9	Gould	400
110	19.33	4.02	18 09 02	−10 11 52	11.8	Gould	408
111	19.50	0.27	18 22 48	−11 50 20	6.0	Gal	406
112	20.63	−4.83	18 43 29	−13 11 55	7.9	Gal	
113	21.17	4.94	18 09 20	−08 08 33	4.7	Gould	422
114	21.25	9.75	17 52 32	−05 45 28	6.6	Gould	421
115	21.27	12.10	17 44 20	−04 35 24	4.0	Gould	425
116	21.70	9.08	17 55 44	−05 41 23	7.9	Gould	432
117	22.18	4.78	18 11 52	−07 20 08	5.3	Gould	436
118	22.33	5.02	18 11 16	−07 05 35	7.3	Gould	438
119	22.35	3.20	18 17 47	−07 56 39	5.3	Gould	437
120	22.38	−1.11	18 33 16	−09 55 55	4.0	Gal	445
121	22.66	−0.11	18 30 11	−09 13 25	4.7	Gal	443
122	22.99	0.69	18 27 58	−08 33 33	7.9	Gal	446
123	23.13	4.87	18 13 21	−06 27 34	5.3	Gould	447
124	23.16	3.28	18 19 02	−07 11 34	8.6	Gould	451
125	23.31	8.45	18 01 02	−04 35 47	7.3	Gould	444
126	23.36	10.04	17 55 32	−03 47 18	6.0	Gould	460
127	23.65	7.57	18 04 47	−04 43 13	7.9	Gould	462
128	23.73	8.40	18 02 01	−04 15 39	7.3	Gould	
129	23.73	0.68	18 29 24	−07 54 24	8.6	Gal	463
130	23.87	4.21	18 17 06	−06 07 26	6.6	Gould	466
131	24.07	2.64	18 23 03	−06 41 23	7.9	Gal	
132	24.35	6.05	18 11 29	−04 49 56	9.2	Gould	469
133	24.41	4.73	18 16 16	−05 24 36	6.6	Gould	476
134	24.45	−3.42	18 45 27	−09 09 40	7.3	Gal	
135	24.89	5.33	18 15 04	−04 42 06	6.0	Gould	483
136	25.24	7.83	18 06 52	−03 13 02	6.6	Gould	
137	25.67	−0.39	18 36 51	−06 40 59	12.5	Gal	497
138	25.78	2.95	18 25 09	−05 01 51	9.2	Gal	
139	26.02	−0.54	18 39 03	−06 26 27	14.4	Gal	499
140	26.36	8.65	18 06 03	−01 51 03	13.8	Gould	502
141	26.47	8.01	18 08 31	−02 03 21	6.0	Gould	
142	26.48	3.28	18 25 18	−04 16 00	2.7	Gould	503
143	26.64	8.32	18 07 46	−01 45 28	6.0	Gould	508
144	26.88	6.89	18 13 16	−02 13 25	7.9	Gould	507
145	27.63	7.99	18 10 45	−01 02 58	6.6	Gould	519
146	27.69	2.11	18 31 43	−03 44 21	10.5	Gal	
147	27.71	5.69	18 19 02	−02 03 21	6.0	Gould	520
148	27.87	5.59	18 19 42	−01 57 46	4.7	Gould	520
149	28.46	−6.44	19 03 39	−06 58 53	11.8	Gal	531
150	28.51	−1.87	18 47 23	−04 51 03	4.0	Gal	530
151	28.84	1.84	18ʰ34ᵐ47ˢ	−2°50′40″	7.9	Gal	538
152	28.84	−1.74	18 47 32	−04 29 48	10.5	Gal	
153	29.12	−1.93	18 48 44	−04 19 44	4.7	Gal	
154	29.23	−4.73	18 58 56	−05 30 55	9.9	Gal	544
155	29.39	−4.83	18 59 33	−05 25 20	11.8	Gal	549
156	29.47	−0.83	18 45 27	−03 30 55	7.9	Gal	548
157	29.68	−0.54	18 44 47	−03 11 55	10.5	Gal	
158	30.34	−1.33	18 48 49	−02 58 29	13.1	Gal	
159	30.42	−4.84	19 01 29	−04 30 55	10.6	Gal	567
160	30.70	−0.43	18 46 17	−02 14 09	7.3	Gal	556
161	31.30	−5.36	19 04 56	−03 57 46	0.8	Gal	581
162	31.43	−1.18	18 50 18	−01 56 15	13.8	Gal	582
163	32.38	−15.30	19 42 32	−07 30 55	3.4	Gal	595
164	32.66	0.46	18 46 44	−00 05 35	9.2	Gal	596
165	33.43	−0.06	18 50 00	00 21 15	9.9	Gal	604
166	34.32	−0.84	18 54 24	00 46 58	13.1	Gal	617
167	34.65	−6.59	19 15 27	−01 34 17	9.2	Gal	619
168	34.75	−5.89	19 13 09	−01 09 40	9.3	Gal	618
169	35.31	6.28	18 30 53	04 55 55	8.6	Gould	
170	35.40	0.04	18 53 17	02 08 57	14.4	Gal	
171	35.51	0.87	18 50 32	02 38 01	10.5	Gal	
172	35.55	−5.16	19 12 02	−00 07 03	9.2	Gal	
173	35.70	−3.09	19 04 56	00 58 29	33.3	Gal	
174	35.79	−5.42	19 13 22	−00 01 27	9.2	Gal	
175	36.95	−2.25	19 04 16	02 27 57	26.8	Gal	
176	36.98	−5.63	19 16 20	00 55 35	9.9	Gal	629
177	37.66	−2.08	19 05 00	03 10 27	6.6	Gal	
178	37.75	−2.25	19 05 45	03 10 27	7.3	Gal	
179	37.87	−5.44	19 17 18	01 48 08	10.6	Gal	
180	38.33	−0.94	19 20 10	04 17 54	17.7	Gal	636
181	39.09	−2.20	19 08 04	04 23 06	31.4	Gal	
182	39.16	−1.04	19 04 06	04 59 16	13.1	Gal	636
183	42.03	2.41	18 57 05	09 07 26	30.1	Gal	
184	42.88	−2.79	19 17 18	07 27 34	7.9	Gal	647
185	43.01	8.37	18 37 15	12 41 23	4.0	Gould	648
186	43.36	2.96	18 57 34	10 33 33	9.9	Gould	
187	43.69	1.43	19 03 43	10 08 57	−22.6	Gal	
188	43.81	−2.42	19 17 45	08 26 50	7.9	Gal	655
189	44.29	−2.40	19 18 35	08 52 34	28.1	Gal	657
190	44.45	−2.67	19 19 51	08 53 41	8.6	Gal	661
191	44.47	−2.47	19 19 11	09 00 23	7.3	Gal	661
192	44.94	−6.55	19 34 33	07 27 57	8.6	Gal	663
193	45.11	3.86	18 57 35	12 30 59	31.4*	Gould	
194	45.27	9.13	18 38 28	15 01 30	6.6	Gould	666
195	45.67	0.27	19 11 40	11 21 15	64.5	Gal	
196	46.27	−1.22	19 18 11	11 11 11	6.0	Gal	673
197	46.51	2.74	19 04 19	13 14 35	26.2	Gal	
198	46.80	−7.73	19 42 22	08 30 12	7.9	Gal	680
199	47.45	−0.86	19 19 10	12 23 29	6.6	Gal	684
200	47.69	−5.57	19 36 27	10 20 08	8.7	Gal	688

TABLE 3—*Continued*

No. (1)	*l* (2)	*b* (3)	R.A. (4)	Decl. (5)	Velocity (6)	Belt (7)	Lynds # (8)
201	47.80	5.08	$18^h58^m09^s$	15°27′57″	13.2	Gould	
202	48.23	−5.73	19 38 06	10 43 37	9.2	Gal	694
203	48.40	−5.87	19 38 57	10 48 05	9.9	Gal	
204	49.07	−4.18	19 34 15	12 12 38	9.8	Gal	702
205	49.22	−4.00	19 33 56	12 26 04	10.6	Gal	705
206	49.26	−1.35	19 24 28	13 44 57	5.3	Gal	704
207	49.49	−2.75	19 29 57	13 16 23	46.3	Gal	
208	49.76	−2.12	19 28 15	13 48 49	11.9	Gal	
209	50.08	2.67	19 11 24	16 22 19	5.4	Gal	709
210	50.22	−1.73	19 27 42	14 23 29	4.7	Gal	
211	51.25	−2.76	19 33 32	14 48 05	17.1	Gal	
212	52.21	2.30	19 16 57	18 05 12	15.1	Gal	
213	53.01	3.07	19 15 40	19 08 57	11.2	Gould	723
214	53.03	1.42	19 21 52	18 23 06	23.5	Gal	722
215	53.15	2.15	19 19 23	18 49 56	23.6	Gal	
216	53.19	0.44	19 25 48	18 02 58	23.6	Gal	725
217	53.56	0.08	19 27 53	18 12 18	22.9	Gal	
218	53.67	0.68	19 25 54	18 35 24	24.2	Gal	
219	53.86	3.00	19 17 38	19 51 27	10.0	Gould	730
220	54.02	−2.33	19 37 40	17 25 43	7.9	Gal	731
221	54.61	2.77	19 20 00	20 25 00	7.3	Gould	735
222	54.64	2.79	19 19 59	20 27 06	27.5*	Gould	
223	54.67	3.14	19 18 44	20 38 25	9.2	Gould	738
224	54.76	3.67	19 16 54	20 58 33	7.3	Gould	732
225	55.14	1.64	19 25 19	20 20 31	10.6	Gal	
226	55.35	3.06	19 20 24	21 12 18	9.2	Gould	746
227	55.51	3.83	19 17 50	21 42 30	8.6	Gould	751
228	55.89	2.08	19 25 13	21 12 38	26.8	Gal	
229	55.90	2.03	19 25 25	21 11 58	9.9	Gal	756
230	56.12	−2.94	19 44 18	18 55 55	15.1	Gal	758
231	56.91	4.82	19 16 51	23 24 36	11.2	Gould	763
232	57.11	4.45	19 18 42	23 24 36	10.6	Gould	771
233	57.12	3.65	19 21 45	23 02 14	11.2	Gould	769
234	57.15	0.57	19 33 29	21 34 40	9.3	Gal	761
235	57.28	4.03	19 20 39	23 21 15	11.2	Gould	774
236	57.29	1.17	19 31 33	22 00 00	10.5	Gal	770
237	57.39	2.43	19 26 59	22 41 23	11.2	Gould	768
238	57.61	−0.53	19 38 35	21 26 27	9.2	Gal	
239	57.63	0.74	19 33 53	22 04 28	12.5	Gal	
240	57.74	0.80	19 33 53	22 12 41	10.5	Gal	776
241	57.99	0.33	19 36 12	22 11 34	4.1	Gal	
242	58.06	3.07	19 25 57	23 35 03	9.9	Gould	778
243	58.21	0.45	19 36 12	22 26 50	37.8	Gal	
244	58.38	3.30	19 25 44	23 58 29	10.6	Gould	782
245	59.06	−0.08	19 40 01	22 54 48	27.4	Gal	
246	59.07	2.73	19 29 24	24 18 37	11.1	Gould	786
247	59.10	−1.59	19 45 46	22 11 11	23.5	Gal	
248	59.92	2.13	19 33 30	24 45 28	10.6	Gal	788
249	60.00	−0.67	19 44 18	23 26 07	6.7	Gal	
250	60.63	2.23	19 34 39	25 25 43	10.6	Gal	790

No. (1)	*l* (2)	*b* (3)	R.A. (4)	Decl. (5)	Velocity (6)	Belt (7)	Lynds # (8)
251	60.65	2.32	$19^h34^m20^s$	25°29′05″	4.1	Gould	790
252	60.66	2.53	19 33 32	25 35 47	11.2	Gould	
253	60.67	−0.30	19 44 24	24 11 55	30.7	Gal	
254	60.74	−1.21	19 47 58	23 47 42	11.2	Gal	791
255	60.94	2.26	19 35 12	25 42 30	10.6	Gal	792
256	61.12	0.74	19 41 28	25 06 43	5.4	Gal	
257	61.19	1.67	19 38 01	25 38 01	11.2	Gal	793
258	61.73	0.04	19 45 30	25 16 46	−8.3	Gal	
259	61.98	2.39	19 37 00	26 40 39	6.0	Gould	794
260	62.58	0.28	19 46 28	26 08 13	7.3	Gal	798
261	62.83	1.85	19 41 00	27 08 36	0.8	Gal	804
262	62.95	1.72	19 41 45	27 11 11	2.1	Gal	807
263	63.06	1.38	19 43 21	27 06 22	2.8	Gal	808
264	64.80	−2.46	20 02 05	26 35 47	8.6	Gal	814
265	65.29	−2.67	20 04 04	26 53 41	6.0	Gal	
266	65.79	−2.64	20 05 10	27 19 24	8.6	Gal	
267	66.05	−3.09	20 07 30	27 18 17	6.0	Gal	
268	68.62	−3.43	20 15 14	29 14 53	9.9	Gould	824
269	69.11	−3.35	20 16 13	29 41 43	9.2	Gould	827
270	69.95	−2.66	20 15 45	30 46 35	3.4	Gould	
271	70.36	1.68	20 13 03	31 40 16	11.2	Gould	
272	70.57	−3.82	20 21 49	30 37 38	3.4	Gould	837
273	70.68	−0.31	20 08 30	32 41 23	9.9	Gould	841
274	70.75	3.81	19 51 54	34 57 02	6.0	Gal	840
275	70.81	−2.17	20 16 08	31 45 51	8.6	Gould	842
276	71.13	−2.99	20 20 10	31 33 33	7.3	Gould	
277	71.84	1.65	20 03 38	34 43 57	0.8	Gould	848
278	71.97	1.85	20 03 11	34 57 22	1.5	Gal	849
279	72.29	1.76	20 04 22	35 10 48	0.8	Gal	853
280	72.41	1.35	20 06 22	35 02 58	−3.7	Gould	856
281	72.54	0.70	20 09 22	34 48 26	6.0	Gould	858
282	73.94	2.48	20 05 50	36 57 02	−0.5	Gal	863
283	74.09	3.42	20 02 16	37 35 03	−5.0	Gal	865
284	74.20	−5.11	20 36 48	32 46 58	11.2	Gould	
285	74.96	−0.12	20 19 00	36 24 13	5.4	Gould	
286	75.50	2.04	20 11 58	38 00 23	8.0	Gal	
287	75.69	2.76	20 09 27	38 33 56	17.7	Gal	
288	75.88	2.03	20 13 06	38 19 24	0.2	Gal	
289	76.52	1.03	20 19 09	38 17 10	16.5	Gould	
290	77.21	3.30	20 11 30	40 07 50	15.1	Gal	880
291	77.74	0.81	20 23 40	39 08 57	3.4	Gould	
292	77.80	0.84	20 23 45	39 13 02	0.8	Gould	
293	78.20	1.27	20 23 09	39 47 42	0.8	Gould	889
294	78.68	2.67	20 18 33	40 59 16	13.2	Gal	888
295	79.22	2.87	20 19 18	41 32 49	8.0	Gal	
296	80.11	2.75	20 22 36	42 12 18	4.7	Gal	900
297	81.97	5.08	20 17 54	45 03 45	0.8	Gal	908
298	82.95	1.53	20 37 12	43 45 51	4.1	Gal	917
299	83.10	−1.76	20 51 40	41 48 26	4.1	Gould	914
300	83.75	−0.80	20 49 55	42 55 32	2.2	Gould	

TABLE 3—*Continued*

No. (1)	*l* (2)	*b* (3)	R.A. (4)	Decl. (5)	Velocity (6)	Belt (7)	Lynds # (8)
301	84.47	−3.66	$21^h04^m10^s$	41°35′00″	8.0	Gould	932
302	84.65	−1.08	20 54 18	43 25 43	3.5	Gould	935
303	84.73	0.44	20 48 08	44 27 57	−2.4	Gould	931
304	84.76	−4.06	21 06 47	41 31 39	6.1	Gould	
305	84.83	−3.70	21 05 35	41 49 33	4.8	Gould	934
306	85.07	−0.17	20 51 57	44 20 31	1.5	Gould	
307	85.12	0.38	20 49 48	44 43 37	−3.0	Gould	936
308	85.19	−3.04	21 04 18	42 32 02	10.6	Gould	
309	85.41	−2.06	21 01 08	43 21 15	2.8	Gould	
310	85.58	−3.51	21 07 35	42 29 48	8.7	Gould	938
311	85.59	−2.62	21 04 05	43 06 43	9.3	Gould	
312	85.61	−4.25	21 10 36	42 00 44	6.7	Gould	
313	86.04	−4.89	21 14 42	41 52 54	8.7	Gould	
314	86.42	0.18	20 55 25	45 35 24	0.9	Gould	941
315	86.63	−1.93	21 05 06	44 20 31	10.6	Gould	
316	86.86	−4.10	21 14 42	43 01 07	4.8	Gould	942
317	86.88	−4.90	21 17 54	42 28 41	8.0	Gould	948
318	86.92	−2.02	21 06 36	44 29 28	11.9	Gould	
319	86.92	−5.12	21 18 54	42 20 51	8.0	Gould	
320	87.04	−2.54	21 09 12	44 13 49	12.6	Gould	
321	87.08	−4.19	21 15 55	43 06 43	2.2	Gould	
322	87.36	−4.23	21 17 09	43 16 46	4.8	Gould	946
323	87.56	−4.38	21 18 29	43 19 01	7.4	Gould	952
324	89.36	−0.69	21 10 38	47 11 11	2.8	Gould	970
325	89.66	−6.63	21 35 19	43 07 50	12.6	Gould	973
326	89.70	2.21	20 59 12	49 23 53	−0.4	Gal	978
327	89.75	−6.93	21 36 45	42 57 46	12.6	Gould	977
328	89.85	−2.00	20 18 07	46 36 54	1.5	Gould	974
329	90.12	2.79	20 58 11	50 05 35	−0.4	Gal	981
330	90.19	−2.16	21 20 12	46 44 44	4.8	Gould	
331	90.43	3.09	20 58 04	50 31 19	−0.4	Gal	985
332	90.46	2.35	21 01 39	50 03 21	−1.1	Gal	984
333	90.52	−1.49	21 18 47	47 27 14	2.8	Gould	989
334	91.16	2.82	21 02 24	50 53 41	−4.3	Gal	998
335	91.65	4.88	20 54 29	52 36 54	−3.0	Gal	1002
336	91.93	4.15	20 59 19	52 21 15	−2.4	Gal	1003
337	92.08	−1.16	21 24 06	48 46 35	4.8	Gould	1007
338	92.27	3.61	21 03 26	52 14 32	−3.0	Gal	1011
339	92.50	4.58	20 59 41	53 03 45	−3.7	Gal	1013
340	92.56	−0.87	21 25 00	49 19 01	4.8	Gould	
341	92.65	−0.13	21 22 14	49 54 48	4.1	Gould	1014
342	93.03	3.37	21 07 58	52 38 01	−2.4	Gal	1022
343	93.25	9.70	20 35 09	56 51 27	−2.4	Gal	1033
344	93.48	8.75	20 41 41	56 27 57	−2.4	Gal	1039
345	93.49	9.51	20 37 16	56 55 55	−2.4	Gal	1033
346	93.53	9.55	20 37 12	56 59 16	−1.7	Gal	1036
347	93.62	−4.45	21 44 06	47 21 15	4.1	Gould	1040
348	93.86	9.97	20 36 11	57 29 48	−2.4	Gal	1041
349	93.88	6.18	20 57 36	55 08 57	−1.1	Gal	
350	94.16	6.23	20 58 38	55 23 29	−1.1	Gal	1053
351	94.16	5.14	$21^h04^m21^s$	54°39′52″	−3.1	Gal	1050
352	94.31	−5.19	21 50 00	47 13 25	6.1	Gould	1055
353	94.46	−5.38	21 51 25	47 10 04	8.7	Gould	
354	94.71	6.26	21 01 00	55 49 12	−1.1	Gal	1058
355	95.23	6.52	21 02 05	56 22 45	−0.4	Gal	1065
356	95.96	3.61	21 03 26	52 14 32	−3.0	Gal	
357	96.37	1.47	21 32 39	53 37 38	2.2	Gal	1074
358	96.41	5.27	21 14 29	56 23 29	0.2	Gal	
359	96.52	2.06	21 30 45	54 10 04	2.2	Gal	1075
360	96.69	1.44	21 34 26	53 48 49	0.9	Gal	1078
361	96.90	2.12	21 32 24	54 27 57	6.1	Gal	1079
362	97.09	10.12	20 50 18	60 06 43	8.0	Gal	1082
363	97.22	9.88	20 52 23	60 03 21	−2.4	Gal	
364	98.30	3.30	21 34 00	56 17 54	7.4	Gal	1087
365	98.38	3.59	21 33 10	56 32 26	8.0	Gal	1090
366	98.54	13.87	20 31 57	63 29 48	−2.4	Gal	1089
367	98.60	2.74	21 38 24	56 03 21	8.0	Gal	1088
368	98.77	2.59	21 40 00	56 03 21	6.7	Gal	
369	99.11	3.95	21 35 21	57 18 17	−8.2	Gal	1105
370	99.12	4.64	21 31 59	57 49 33	−5.0	Gal	1102
371	99.13	2.87	21 40 40	56 30 12	4.1	Gal	1104
372	99.38	4.06	21 36 21	57 33 53	1.5	Gal	
373	99.61	4.14	21 37 12	57 46 11	−0.4	Gal	1112
374	99.65	3.85	21 38 53	57 35 03	−0.4	Gal	1111
375	99.68	2.00	21 47 43	56 11 11	−2.4	Gal	1114
376	100.02	8.87	21 13 33	61 27 57	1.5	Gal	1125
377	100.38	8.82	21 15 53	61 41 23	0.2	Gal	
378	100.78	5.17	21 38 42	59 19 01	−1.1	Gal	1131
379	102.04	15.31	20 39 15	67 05 35	2.2	Gal	1148
380	102.19	3.27	21 56 33	58 44 21	−1.1	Gal	1143
381	102.23	8.31	21 30 09	62 36 54	2.8	Gal	1145
382	102.26	15.95	20 35 02	67 38 01	3.5	Gal	1152
383	102.37	3.02	21 58 51	58 38 45	−2.4	Gal	1153
384	102.40	2.70	22 00 26	58 24 13	−1.0	Gal	1151
385	102.40	−0.54	22 14 12	55 45 28	−6.9	Gould	1150
386	102.46	8.56	21 30 09	62 57 02	2.8	Gal	
387	102.57	−0.36	22 14 29	56 00 00	−5.6	Gal	1154
388	102.67	15.35	20 42 35	67 36 54	0.9	Gal	1158
389	103.10	−15.17	23 01 45	43 15 39	3.5	Gould	
390	103.14	−17.13	23 06 15	41 29 05	−8.2	Gould	
391	103.24	2.76	22 05 23	58 56 39	−1.7	Gal	1164
392	103.75	13.83	21 01 51	67 30 12	2.8	Gal	1172
393	104.24	14.31	21 01 15	68 10 27	2.8	Gal	1174
394	105.07	13.28	21 15 14	58 05 35	2.8	Gal	1177
395	105.57	10.38	21 39 50	66 21 59	−10.8	Gal	1183
396	105.60	1.15	22 27 33	58 53 41	−1.7	Gal	1185
397	106.40	0.43	22 35 40	58 40 16	−3.0	Gal	1197
398	106.45	11.94	21 35 38	68 05 59	−11.5	Gal	1199
399	106.89	5.32	22 18 22	63 07 06	−8.2	Gal	1201
400	107.01	16.78	20 58 36	71 48 05	−5.6	Gal	

TABLE 3—*Continued*

No. (1)	*l* (2)	*b* (3)	R.A. (4)	Decl. (5)	Velocity (6)	Belt (7)	Lynds # (8)	No. (1)	*l* (2)	*b* (3)	R.A. (4)	Decl. (5)	Velocity (6)	Belt (7)	Lynds # (8)
401	107.20	5.22	22ʰ21ᵐ08ˢ	63°12′18″	−11.5	Gal	1201	451	117.96	4.83	23ʰ57ᵐ20ˢ	66°55′32″	−13.9	Gal	1266
402	107.28	−0.30	22 44 14	58 26 50	−3.0	Gal	1200	452	118.16	13.05	23 35 11	74 57 02	−3.0	Gal	
403	107.35	4.46	22 25 45	62 38 01	−5.6	Gal	1202	453	118.31	4.88	00 00 45	67 02 14	−7.1	Gal	1271
404	107.37	4.72	22 24 45	62 52 10	−4.3	Gal	1203	454	118.33	8.69	23 52 19	70 46 35	−2.4	Gal	1274
405	107.51	4.51	22 26 44	62 45 28	−1.0	Gal	1204	455	118.59	6.32	00 00 49	68 30 35	−0.3	Gal	1273
406	108.50	18.15	20 55 41	73 45 51	−6.9	Gal		456	118.64	3.75	00 05 59	65 58 53	−5.8	Gal	
407	109.40	6.71	22 31 12	65 36 54	−8.5	Gal	1213	457	119.22	7.82	00 04 45	70 05 35	−6.3	Gal	
408	109.72	2.54	22 51 35	62 04 52	−9.5	Gal	1216	458	119.82	7.61	00 11 57	69 58 53	−3.0	Gal	
409	109.75	1.92	22 54 07	61 32 26	−11.5	Gal	1218	459	120.72	−1.44	00 30 10	61 04 28	−18.6	Gal	
410	110.34	11.41	22 12 36	70 04 28	−5.1	Gal	1217	460	120.95	−3.83	00 33 13	58 42 27	−17.3	Gould	1286
411	110.41	−12.63	23 34 39	48 08 57	−7.5	Gould		461	121.03	−9.97	00 36 12	52 34 40	−11.4	Gould	
412	110.52	−12.60	23 35 13	48 12 18	−7.5	Gould		462	121.16	0.77	00 32 36	63 18 40	−17.3	Gal	1287
413	110.58	2.28	22 59 12	62 12 18	−10.8	Gal		463	121.36	0.68	00 34 24	63 14 12	−17.3	Gal	1287
414	110.60	11.96	22 11 21	70 40 16	−4.4	Gal	1219	464	121.75	0.23	00 38 01	62 48 29	−17.3	Gal	
415	110.61	−12.57	23 35 39	48 15 39	−8.2	Gould		465	121.87	0.55	00 39 00	63 07 29	−18.0	Gal	1293
416	110.64	9.71	22 26 03	68 49 12	−4.4	Gal	1221	466	121.89	−10.44	00 41 51	52 08 57	−9.8	Gould	1295
417	111.32	9.32	22 34 09	68 54 48	−7.8	Gal		467	121.94	−0.87	00 40 00	61 42 30	5.1	Gal	1294
418	111.39	2.01	23 06 31	62 16 46	−10.2	Gal		468	121.95	−1.58	00 40 19	61 00 00	−14.6	Gal	1298
419	111.44	1.03	23 10 00	61 23 29	−1.2	Gal	1226	469	121.99	−0.54	00 40 19	62 02 38	−11.9	Gal	
420	111.57	14.25	22 03 47	73 04 28	−1.7	Gal		470	122.15	−10.39	00 43 33	52 12 18	−10.5	Gould	1295
421	111.71	13.80	22 08 53	72 47 42	−3.7	Gal		471	122.18	−0.15	00 41 54	62 26 07	−18.0	Gal	1301
422	111.80	1.29	23 12 04	61 45 51	−6.3	Gal	1229	472	122.25	−10.22	00 44 09	52 22 22	−10.5	Gould	1295
423	111.85	1.72	23 11 06	62 11 11	−10.2	Gal	1227	473	122.77	9.64	00 46 01	72 14 32	3.1	Gal	
424	111.99	0.46	23 16 00	61 03 21	−11.2	Gal	1231	474	122.79	−1.19	00 47 14	61 24 36	−18.6	Gal	1300
425	112.12	1.64	23 12 30	62 12 41	−9.2	Gal	1234	475	123.87	−0.80	00 56 21	61 46 58	3.8	Gal	
426	112.22	13.86	22 13 59	73 07 50	−3.7	Gal	1235	476	124.35	2.68	01 01 53	65 14 56	−10.5	Gal	1307
427	113.36	1.61	23 23 36	62 36 11	−11.9	Gal	1244	477	124.61	2.12	01 04 00	64 40 16	−7.8	Gal	
428	113.40	15.62	22 12 44	75 13 49	−5.1	Gal	1243	478	124.87	−0.50	01 04 56	62 02 38	3.8	Gal	1309
429	113.58	2.28	23 23 36	63 18 40	−11.2	Gal	1246	479	125.44	−0.46	01 09 51	62 02 38	−14.0	Gal	
430	113.66	15.04	22 21 05	74 53 41	−5.1	Gal	1247	480	125.53	−1.19	01 18 19	61 12 18	−12.5	Gal	1313
431	114.13	14.84	22 28 34	74 58 09	−3.7	Gal	1251	481	125.64	−0.59	01 11 25	61 53 41	−9.1	Gal	1312
432	114.22	6.15	23 16 57	67 10 04	−7.6	Gal		482	125.71	−1.02	01 11 41	61 27 57	−11.9	Gal	
433	114.34	−2.73	23 41 36	58 44 21	−3.0	Gould	1249	483	125.96	−1.12	01 13 41	61 20 08	−11.2	Gal	1313
434	115.28	1.09	23 40 59	62 40 19	−3.6	Gal		484	126.63	−0.71	01 19 41	61 40 16	−15.3	Gal	1317
435	115.44	1.76	23 40 48	63 21 38	−3.7	Gal		485	126.97	−1.07	01 22 09	61 16 46	−11.9	Gal	1323
436	115.69	1.22	23 44 06	62 53 41	1.7	Gal	1252	486	127.34	13.51	01 57 32	75 32 02	3.1	Gal	
437	115.69	−3.16	23 52 29	58 38 01	−1.0	Gould		487	127.57	13.97	02 03 04	75 54 24	3.8	Gal	
438	115.75	1.26	23 44 36	62 57 05	−8.2	Gal		488	127.88	2.66	01 35 04	64 49 12	−11.2	Gal	1330
439	115.81	−1.97	23 51 21	59 49 36	−1.7	Gould	1255	489	128.85	13.81	02 21 05	75 21 15	3.8	Gal	1333
440	115.82	−3.54	23 54 04	58 17 30	−0.4	Gould	1253	490	128.90	4.41	01 48 11	66 20 08	−2.3	Gal	1336
441	115.98	−3.28	23 45 48	58 34 40	0.4	Gould	1254	491	128.93	−0.20	01 39 32	61 49 12	−14.6	Gal	1332
442	116.02	1.73	23 45 54	63 28 21	−6.9	Gal		492	129.95	11.61	02 24 08	72 54 48	−13.9	Gal	
443	116.08	−2.40	23 54 12	59 27 57	−1.0	Gould	1257	493	130.08	11.48	02 25 09	72 44 44	−15.3	Gal	1340
444	116.10	1.42	23 47 13	63 11 38	−7.5	Gal		494	132.34	13.25	03 03 01	73 22 22	17.4	Gal	
445	116.22	−2.54	23 55 30	59 21 15	−0.4	Gould	1258	495	133.04	0.96	02 15 43	61 51 27	−38.7	Gal	1354
446	116.33	12.29	23 13 56	73 38 45	3.1	Gal	1259	496	133.53	8.58	02 48 21	68 42 30	−3.7	Gal	1357
447	117.12	12.40	23 23 47	74 01 07	3.7	Gal	1262	497	133.57	1.07	02 20 19	61 46 58	−39.4	Gal	1359
448	117.44	12.37	23 24 03	74 00 00	3.7	Gal	1261	498	134.01	0.79	02 22 56	61 22 22	−49.1	Gal	1361
449	117.78	4.17	23 56 53	66 14 32	−5.8	Gal	1266	499	136.36	0.71	02 40 28	60 23 29	−13.9	Gal	1376
450	117.83	9.58	23 43 48	71 31 19	−2.4	Gal		500	136.91	1.17	02 46 10	60 34 40	−39.4	Gal	

TABLE 3—*Continued*

No. (1)	*l* (2)	*b* (3)	R.A. (4)	Decl. (5)	Velocity (6)	Belt (7)	Lynds # (8)	No. (1)	*l* (2)	*b* (3)	R.A. (4)	Decl. (5)	Velocity (6)	Belt (7)	Lynds # (8)
501	137.97	0.85	$02^h52^m40^s$	59°48′49″	−38.1	Gal		551	155.98	4.92	$04^h50^m28^s$	51°23′29″	4.5	Gal	1436
502	138.00	1.77	02 56 18	60 36 54	−42.6	Gal		552	156.08	6.05	04 56 34	52 01 30	5.9	Gal	1439
503	139.87	1.43	03 08 00	59 25 00	−11.2	Gal		553	156.21	5.25	04 53 04	51 25 43	5.2	Gal	1438
504	140.07	0.80	03 06 50	58 45 51	−13.9	Gal		554	157.19	−8.72	03 58 35	41 00 23	−7.1	Gould	1443
505	140.28	2.27	03 14 11	59 55 11	−13.2	Gal	1383	555	157.35	−1.09	04 28 30	46 23 29	5.2	Gal	1445
506	140.76	2.28	03 17 29	59 40 39	−12.5	Gal	1385	556	157.75	−8.86	04 00 16	40 32 26	−5.7	Gould	1447
507	140.78	0.87	03 11 51	58 27 57	0.3	Gal		557	157.88	−8.66	04 01 27	40 35 47	−5.0	Gould	1447
508	141.34	1.38	03 17 33	58 35 47	−9.8	Gal		558	157.90	−8.95	04 00 32	40 22 22	−5.7	Gould	1447
509	141.49	1.42	03 18 42	58 33 33	−10.5	Gal		559	158.30	−8.29	04 04 25	40 35 47	−7.1	Gould	
510	141.78	2.58	03 25 30	59 21 38	−11.2	Gal		560	159.55	11.35	05 37 42	52 10 04	2.4	Gal	1460
511	142.23	0.70	03 20 25	57 33 10	−15.2	Gal		561	159.72	−11.93	03 57 12	36 57 02	1.1	Gould	1462
512	142.62	1.73	03 27 12	58 11 11	−12.5	Gal		562	159.84	−12.10	03 57 07	35 44 44	−33.5*	Gould	1463
513	142.86	1.31	03 26 54	57 42 06	−8.2	Gal		563	159.99	1.12	04 48 11	45 53 17	4.5	Gal	1465
514	143.46	1.51	03 31 24	57 32 02	−9.8	Gal		564	160.62	−1.24	04 40 24	43 52 34	−17.2	Gal	
515	145.41	9.68	04 26 12	62 25 43	−12.7	Gal		565	162.39	−8.75	04 17 48	37 27 34	−0.3	Gould	
516	145.76	7.31	04 14 00	60 31 19	−10.5	Gal		566	162.76	1.39	04 59 10	43 54 24	1.1	Gal	1477
517	145.89	17.78	05 30 11	66 50 20	0.4	Gal		567	163.25	−5.14	04 34 09	39 19 01	−0.3	Gal	1481
518	148.66	2.11	04 03 18	54 45 28	1.8	Gal	1390	568	165.49	−9.08	04 27 06	35 01 07	−0.2	Gould	
519	148.78	2.73	04 06 49	55 07 50	1.8	Gal		569	167.27	−4.24	04 50 54	36 52 10	5.9	Gal	1488
520	149.20	3.04	04 10 27	55 04 28	3.1	Gal	1392	570	167.91	−19.09	04 01 26	26 20 31	7.2	Gould	1489
521	149.35	2.72	04 09 41	54 44 21	2.4	Gal	1393	571	168.06	−19.21	04 01 32	26 09 20	6.8	Gould	1491
522	149.46	3.42	04 13 35	55 10 04	3.1	Gal	1394	572	168.08	−3.35	04 56 52	36 47 42	4.9	Gal	
523	149.58	3.54	04 14 48	55 10 27	3.8	Gal		573	168.15	−15.58	04 13 23	28 29 08	7.9	Gould	
524	149.94	2.74	04 12 44	54 20 51	3.6	Gal		574	168.26	−16.12	04 11 58	28 12 18	6.6	Gould	1495
525	150.34	3.97	04 20 39	54 57 02	3.1	Gal	1399	575	169.00	−15.41	04 16 31	28 11 11	7.2	Gould	
526	150.79	4.14	04 23 38	54 44 44	3.1	Gal	1403	576	169.20	−14.90	04 18 48	28 23 29	7.2	Gould	
527	150.91	4.64	04 26 45	55 00 23	2.5	Gal	1404	577	169.43	−16.19	04 15 15	27 20 51	5.2	Gould	1495
528	151.11	4.47	04 26 53	54 44 44	3.1	Gal		578	169.51	−18.50	04 08 04	25 41 23	7.9	Gould	
529	151.14	4.91	04 29 14	55 01 30	2.4	Gal	1405	579	169.83	−16.14	04 16 38	27 05 59	5.9	Gould	
530	151.48	3.97	04 26 05	54 07 50	1.8	Gal	1407	580	169.86	−19.41	04 06 13	24 48 49	7.9	Gould	
531	151.57	4.99	04 31 41	54 45 51	−6.4	Gal	1409	581	170.08	−18.98	04 08 12	24 57 46	7.9	Gould	1498
532	151.71	5.09	04 32 51	54 43 37	−6.2	Gal	1410	582	170.90	−18.33	04 12 39	24 51 03	7.9	Gould	1501
533	151.85	4.99	04 32 59	54 33 33	−7.1	Gal	1411	583	171.87	−5.24	05 00 55	32 39 08	7.2	Gal	1512
534	151.99	4.75	04 32 24	54 17 54	4.5	Gal	1412	584	172.19	−16.95	04 20 48	24 53 41	7.2	Gould	
535	152.16	3.20	04 25 33	53 06 19	−8.2	Gal		585	172.36	−8.11	04 51 42	30 30 12	5.2	Gould	1517
536	152.38	−1.73	04 04 40	49 24 36	6.2	Gal		586	172.40	−7.90	04 52 34	30 35 47	5.9	Gould	1517
537	152.46	3.91	04 30 22	53 23 06	−7.1	Gal	1414	587	172.73	−4.85	05 04 49	32 12 18	7.2	Gal	1522
538	152.56	5.31	04 37 51	54 14 32	−5.7	Gal	1415	588	172.74	−14.56	04 30 17	26 04 52	5.9	Gould	1521
539	154.02	5.10	04 43 11	53 00 47	3.8	Gal	1426	589	172.95	−5.48	05 03 05	31 38 45	7.2	Gal	1523
540	154.07	2.18	04 29 19	51 01 30	−2.3	Gal		590	173.37	−13.76	04 34 45	26 08 13	5.9	Gould	
541	154.14	5.24	04 44 26	53 00 47	3.8	Gal	1426	591	173.46	2.88	05 37 36	35 58 53	−19.8	Gal	1525
542	154.35	2.70	04 32 53	51 10 27	−2.3	Gal		592	173.49	−13.37	04 36 24	26 18 17	5.9	Gould	1527
543	154.76	2.65	04 34 25	50 50 20	2.5	Gal		593	173.64	−16.25	04 27 09	24 19 01	6.6	Gould	1524
544	154.97	4.64	04 44 55	51 59 16	3.1	Gal	1431	594	174.19	−13.93	04 36 28	25 25 43	5.2	Gould	1534
545	155.26	3.72	04 41 37	51 10 27	−2.3	Gal		595	174.46	−13.52	04 38 37	25 29 05	5.9	Gould	1532
546	155.36	4.90	04 47 40	51 51 27	5.2	Gal	1432	596	174.49	−15.73	04 31 15	24 02 14	6.6	Gould	
547	155.37	3.65	04 41 45	51 02 38	−1.6	Gal		597	174.71	−15.49	04 32 38	24 02 14	5.9	Gould	1535
548	155.47	−14.58	03 32 41	37 31 19	1.8	Gould	1434	598	174.87	−12.71	04 42 31	25 41 23	5.5	Gould	
549	155.67	5.12	04 50 14	51 45 51	4.5	Gal	1436	599	175.19	−16.73	04 29 50	22 52 34	5.9	Gould	1536
550	155.90	5.28	04 51 56	51 41 23	5.2	Gal	1436	600	175.46	−12.21	04 45 50	25 33 33	5.2	Gould	

TABLE 3—*Continued*

No. (1)	*l* (2)	*b* (3)	R.A. (4)	Decl. (5)	Velocity (6)	Belt (7)	Lynds # (8)
601	175.59	−16.71	04h30m57s	22°35′47″	5.9	Gould	
602	175.97	−9.64	04 56 14	26 45 07	7.2	Gould	
603	176.37	−10.68	04 53 37	25 48 05	6.8	Gould	
604	176.46	−9.83	04 56 51	26 14 56	7.2	Gould	1540
605	177.20	−15.15	04 40 26	22 23 26	−39.3*	Gould	
606	177.85	−9.77	05 00 44	25 11 11	7.2	Gould	1544
607	178.50	−6.77	05 13 11	26 25 43	7.2	Gould	1547
608	178.68	−7.04	05 12 41	26 07 50	7.2	Gould	1548
609	178.90	−6.73	05 14 21	26 07 50	7.2	Gould	1549
610	180.82	4.40	06 01 49	30 26 50	2.5	Gal	1557
611	182.16	−17.94	04 43 32	16 55 55	9.3	Gould	1558
612	189.34	3.89	06 18 04	22 44 44	−1.6	Gal	1568
613	191.18	−16.65	05 08 15	10 36 54	1.8	Gould	1572
614	191.50	−0.70	06 05 19	18 39 08	−0.2	Gal	1574
615	192.01	−0.84	06 05 51	18 07 50	−0.2	Gal	1578
616	192.25	−11.32	05 28 56	12 35 47	10.0	Gould	1582
617	194.54	−15.76	05 18 17	08 22 22	−0.2	Gould	1588
618	195.14	−16.43	05 17 13	07 32 02	−0.2	Gould	1590
619	195.15	−16.91	05 15 35	07 16 23	−2.3	Gould	1589
620	196.14	−2.87	06 06 51	13 32 26	−36.1	Gal	1591
621	196.93	−15.54	05 23 53	06 31 19	−40.6*	Gould	1595
622	196.97	−10.36	05 41 59	09 07 06	12.0	Gould	1594
623	204.41	−11.20	05 53 26	02 20 08	1.1	Gould	1621
624	204.44	−11.30	05 53 08	02 15 39	1.1	Gould	
625	204.52	−10.96	05 54 29	02 21 15	1.6	Gould	1624
626	204.66	−11.71	05 52 06	01 52 10	1.1	Gould	1622
627	204.83	−11.48	05 53 13	01 50 20	1.6	Gould	1624
628	205.25	−14.38	05 43 49	00 05 59	9.3	Gould	1627
629	206.15	−15.76	05 40 36	−01 19 01	9.3	Gould	1630
630	206.45	1.30	06 41 33	06 24 36	15.3	Gal	1631
631	206.52	−16.33	05h39m15s	−01°54′24″	10.0	Gould	
632	207.31	−16.46	05 40 13	−02 38 01	8.8	Gould	1635
633	207.36	−1.22	06 34 15	04 26 50	10.0	Gal	
634	207.65	−1.86	06 32 32	03 53 17	14.0	Gal	
635	207.93	−16.42	05 41 29	−03 08 33	10.7	Gould	1636
636	208.17	−19.54	05 30 49	−04 47 18	10.7	Gould	
637	208.45	−18.71	05 34 15	−04 38 22	6.8	Gould	
638	209.54	−18.65	05 36 21	−05 32 02	7.3	Gould	
639	209.95	−19.37	05 34 29	−06 12 18	8.6	Gould	
640	210.63	−19.57	05 34 56	−06 52 10	7.3	Gould	1641
641	210.86	−19.18	05 36 43	−06 53 17	7.3	Gould	
642	211.61	−19.02	05 38 36	−07 26 50	5.9	Gould	
643	212.49	−19.00	05 40 09	−08 10 48	3.2	Gould	
644	212.86	−19.38	05 39 24	−08 39 52	5.2	Gould	
645	212.89	−12.44	06 04 29	−05 35 47	12.7	Gould	1644
646	212.94	−12.30	06 05 04	−05 34 40	12.7	Gould	1645
647	214.91	−12.80	06 06 46	−07 30 55	11.3	Gould	
648	215.67	−12.89	06 07 45	−08 13 25	6.2	Gould	
649	219.00	−8.75	06 28 39	−09 18 26	11.3	Gould	
650	219.38	−9.54	06 26 27	−10 00 00	4.9	Gould	
651	219.65	−10.78	06 22 26	−10 46 58	4.8	Gould	
652	223.48	−1.79	07 02 03	−10 07 26	18.8	Gal	1657
653	224.31	−0.77	07 07 17	−10 23 06	14.7	Gal	
654	224.42	−2.36	07 01 44	−11 13 02	9.3	Gal	
655	225.05	−2.73	07 01 35	−11 56 39	10.6	Gal	
656	227.82	5.36	07 35 59	−10 33 10	−26.4	Gal	
657	232.71	1.03	07 30 13	−16 55 32	17.2	Gal	
658	236.35	−4.87	07 15 33	−22 56 15	7.9	Gal	1659
659	237.35	−4.74	07 18 03	−23 45 28	19.5	Gal	1660
660	238.39	−4.14	07 22 31	−24 23 29	20.1	Gal	1664
661	238.93	−1.65	07 33 12	−23 39 29	18.8	Gould	1665
662	240.05	−1.81	07 35 00	−24 43 13	17.4	Gould	1668

REFERENCES

Allen, C. W. 1976, *Astrophysical Quantities* (3d ed.; London: Athlone Press).
Bonneau, M. 1964, *J. Obs.*, **47**, 251.
Bruhweiler, F. C., Gull, T. R., Kafatos, M., and Sofia, S. 1980, *Ap. J.* (*Letters*), **238**, L27.
Clemens, D. 1985, *Ap. J.*, **295**, 422.
Cox, D. P. 1979, *Ap. J.*, **234**, 863.
Dickman, R. L. 1975, *Ap. J.*, **202**, 50.
Dickman, R. L., and Kleiner, S. C. 1985, *Ap. J.*, **295**, 479.
Dixon, R. S., Gearhart, M. R., and Schmidtke, P. C. 1981, *Atlas of Sky Overlay Maps* (*For the Palomar Sky Survey*) (Columbus: Ohio State University Radio Observatory).
Eggen, O. J. 1961, *Royal Obs. Bull.*, No. 41.
Elias, J. H. 1978, *Ap. J.*, **224**, 847.
Feitzinger, J. V., and Stüwe, J. A. 1984, *Astr. Ap. Suppl.*, **58**, 365.
———. 1986, *Ap. J.*, **305**, 534.
Frogel, J. A., and Stothers, R. 1977, *A.J.*, **82**, 890 (FS).
Gottlieb, D. M., and Upson, W. L. 1969, *Ap. J.*, **157**, 611.
Goulet, T. 1984, Master's thesis, University of British Columbia.
Hughes, V. A., and Routledge, D. 1972, *A. J.*, **77**, 210.
Lesh, J. R. 1968, *Ap. J. Suppl.*, **17**, 371.
Lindblad, P. O. 1967, *Bull. Astr. Inst. Netherlands*, **19**, 34 (Paper 1).
Lindblad, P. O., Grape, K., Sandquist, Aa., and Schober, J. 1973, *Astr. Ap.*, **24**, 309.
Lynds, B. T. 1962, *Ap. J. Supp.*, **7**, 1.
———. 1968, in *Stars and Stellar Systems*, Vol. **7**, *Nebulae and Interstellar Matter*, ed. B. M. Middlehurst and L. H. Aller (Chicago: University of Chicago Press).
Machnik, D. E., Hettrick, M. C., Kutner, M. L., Dickman, R. L., and Tucker, K. D. 1980, *Ap. J.*, **242**, 121.
Magnani, L., Blitz, L., and Mundy, L. 1985, *Ap. J.*, **295**, 402.
Olano, C. A. 1982, *Astr. Ap.*, **112**, 195.
Oort, J. H. 1927, *Bull. Astr. Inst. Netherlands*, **3**, 275.
Penzias, A. A., and Burrus, C. A. 1973, *Ann. Rev. Astr. Ap.*, **11**, 51.
Sanders, D. B., Solomon, P. M., and Scoville, N. Z. 1984, *Ap. J.*, **276**, 182.
Shuter, W. L. H. 1982, *M.N.R.A.S.*, **199**, 109.
Spitzer, L. 1978, *Physical Processes in the Interstellar Medium* (New York: Wiley).
Stothers, R., and Frogel, J. A. 1974, *A.J.*, **79**, 456 (SF).
Wilking, B. A., and Lada, C. J. 1983, *Ap. J.*, **274**, 698.

R. L. DICKMAN and DAVID K. TAYLOR: Five College Radio Astronomy Observatory, University of Massachusetts, Amherst, MA 01003

N. Z. SCOVILLE: Astronomy Department, 105–24, California Institute of Technology, Pasadena, CA 91125